Published in final edited form as:
J Comp Neurol. 1995 May 1; 355(2): 296–315. doi:10.1002/cne.903550208.

Characterization of Inducible Cyclooxygenase in Rat Brain

CHRISTOPHER D. BREDER[1], **DAVID DEWITT**[3], and **RICHARD P. KRAIG**[1,2]

[1] Department of Neurology, The University of Chicago, Chicago, Illinois 60637

[2] Department of Pharmacological and Physiological Sciences, The University of Chicago, Chicago, Illinois 60637

[3] Department of Biochemistry, Michigan State University, East Lansing, Michigan 48824

Abstract

Considerable debate exists regarding the cellular source of prostaglandins in the mammalian central nervous system (CNS). At least two forms of prostaglandin endoperoxide synthase, or cyclooxygenase (COX), the principal enzyme in the biosynthesis of these mediators, are known to exist. Both forms have been identified in the CNS, but only the distribution of COX 1 has been mapped in detail. In this study, we used Western blot analysis and immunohistochemistry to describe the biochemical characterization and anatomical distribution of the second, mitogen-inducible form of this enzyme, COX 2 in the rat brain.

COX 2-like immunoreactive (COX 2-ir) staining occurred in dendrites and cell bodies of neurons, structures that are typically postsynaptic. It was noted in distinct portions of specific cortical laminae and subcortical nuclei. The distribution in the CNS was quite different from COX 1. COX 2-ir neurons were primarily observed in the cortex and allocortical structures, such as the hippocampal formation and amygdala. Within the amygdala, neurons were primarily observed in the caudal and posterior part of the deep and cortical nuclei. In the diencephalon, COX 2-ir cells were also observed in the paraventricular nucleus of the hypothalamus and in the nuclei of the anteroventral region surrounding the third ventricle, including the vascular organ of the lamina terminalis. COX 2-ir neurons were also observed in the subparafascicular nucleus, the medial zona incerta, and pretectal area. In the brainstem, COX 2-ir neurons were observed in the dorsal raphe nucleus, the nucleus of the brachium of the inferior colliculus, and in the region of the subcoeruleus. The distribution of COX 2-ir neurons in the CNS suggests that COX 2 may be involved in processing and integration of visceral and special sensory input and in elaboration of the autonomic, endocrine, and behavioral responses.

Indexing terms

prostaglandins; hippocampus; amygdala; hypothalamus; immunohistochemistry

Prostaglandins are thought to play a role in several nervous system functions including control of the sleep–wake cycle (Hayaishi, 1991), the generation of fever (Stitt, 1991), transmission of pain (Horiguchi et al., 1986), regulation of the autonomic nervous system (Hedqvist, 1977), and hypothalamic regulation of pituitary function (Ojeda et al., 1982). The principal enzyme in prostaglandin biosynthesis is prostaglandin endoperoxide synthase or cyclooxygenase (COX; Smith et al., 1991). Until recently, only one form of this enzyme, COX 1, had been purified and cloned (Dewitt and Smith, 1990). The distribution of this enzyme in the ovine central nervous system (CNS) has been mapped in detail (Breder et al., 1992). COX

Address reprint requests to Dr. Richard Kraig, Department of Neurology, MC2030, University of Chicago, 5841 S. Maryland Ave., Chicago, IL 60637.

1-like immunoreactive (-ir) neurons were observed in areas involved in complex integrative processes, central autonomic regulation, and sensory afferent transmission.

A novel, inducible form of this enzyme has been cloned and is called COX 2 (Xie et al., 1991). Yamagata et al. (1993) showed that this form is present in neurons of the cortex, hippocampus, and amygdala. They also showed that COX 2 mRNA and protein was induced by stressful and physiological activity.

In this study we used an affinity-purified polyclonal antiserum raised against a unique peptide sequence of COX 2 to stain the normal rat brain. We also observed COX 2-ir neurons in the cortex, hippocampus, and amygdala. Our data show that the enzyme is not diffusely distributed in these structures but is discretely organized. Furthermore, we observed an extensive distribution of COX 2-ir neurons in the diencephalon and brainstem, particularly in nuclei involved in special sensory processing (Tork et al., 1979) or autonomic regulation (Loewy, 1990). Our data suggest that COX 2 is involved in polymodal sensory integration and in the generation of the autonomic, endocrine, and behavioral responses.

MATERIALS AND METHODS

Preparation of the antiserum

Preparation and characterization of the antiserum against murine COX 2 have been described elsewhere (Dewitt and Meade, 1993). This peptide corresponds to a carboxy terminal sequence that is unique from that of COX 1. Briefly, rabbits were immunized with a 17-mer peptide (termed DD-2) conjugated to keyhole limpet hemocyanin. The resulting antiserum was affinity purified with the synthetic peptide conjugated to SulfoLink coupling gel (Pierce; Regier et al., 1993). This antiserum recognizes murine COX 2 but not COX 1 in Western blot analysis.

Western blot analysis

Western blot analysis was performed according to methods of Dewitt and Meade (1993). Briefly, microsomes were prepared from rat brain cortex (where we observed many COX 2-ir neurons) and from the cerebellum (where only background staining was noted). Microsomes were also prepared from unstimulated and lipopolysaccharide (LPS)-stimulated RAW 243.7 cells. Protein (100 μg) was separated by sodium dodecyl sulfate polyacrilamide gel electrophoresis (SDS-PAGE) on 0.45 μm nitrocellulose (Schleicher & Schuell). Membranes were blocked with 3% (v/v) dried milk in Tris buffered saline (TBS) and hybridized for 6–8 hours at 4°C with the primary antibody diluted in 1% dried milk in TBS. Membranes were washed and incubated with a goat anti-rabbit IgG conjugated to horseradish peroxidase. Blots were developed by ECL chemiluminescence (Amersham) on XAR-5 film (Kodak) according to the manufacturer's instructions.

Tissue preparation

Male Wistar rats were maintained in individual cages with access to food and water ad libitum in a room maintained at 22°C with a 12-hour nightlday cycle. Twelve 250–300-gm rats were deeply anesthetized with halothane and perfused transcardially with 150–300 ml of 150 mM NaCl followed by 500 ml of 2% paraformaldehyde/0.075 M lysine-HCl in 0.037 M phosphate buffer, pH 6.2. The brains were removed and cut into 1-cm blocks and postfixed in the fixative solution for 2 hours at 4°C. Brain were then placed in 10% sucrose in 0.1 M phosphate buffer, pH 7.4, for about 12 hours and then 20% sucrose in 0.1 M phosphate buffer for 24 hours. The brains were frozen in isopentane cooled to −30°C and stored in plastic bags at −72°C until cut. Blocks were frozen onto chucks, and sections were cut at 40 μm into 10 adjacent series on a cryostat microtome (Reichert). Sections were stored in 0.1 mM phosphate buffered 0.9% saline (PBS), pH 7.4, at 4°C until ready for use.

Immunohistochemistry

The tissue was stained with an indirect immunoperoxidase technique identical to that described in Breder et al. (1993). Three complete series of sections were incubated in PBS containing 3% H_2O_2 and 0.25% Triton X-100 for 30 minutes and then washed 3 × 5 minutes in PBS (150 mM NaCl and 0.1 M phosphate buffer, pH 7.2). Sections were then incubated for 1 hour at room temperature in a blocking solution containing 3% normal goat serum (Colorado Serum Co.) and 0.25% Triton X-100. The tissue was gently shaken overnight in the primary antiserum diluted 1:750 in the blocking solution. Approximately 18 hours later, the sections were washed in PBS and incubated for 1 hour at room temperature in the secondary antibody, a goat anti-rabbit IgG conjugated to horseradish peroxidase in blocking solution (1:100; Biosource Intl., also from Vector). Sections were washed in PBS and incubated for 7 minutes at room temperature in 0.05% diaminobenzidine dihydro-chloride (DAB; Sigma) and 0.01% H_2O_2 in 0.1 M phosphate buffer. Sections were washed in PBS, mounted onto gelatin/chrome-alum subbed slides, dehydrated in a series of graded ethanols, and cleared in xylene.

One complete series was coverslipped with DPX (BDH Limited; Poole, England) after 24 hours of clearing. Two series were intensified with a silver–gold intensification procedure (Breder et al., 1992).

Preadsorption of the antiserum

Specificity of the antisera was tested by preadsorbing 1 ml of the primary antiserum with 5 μM of the DD-2 peptide. Adjacent sections from the rat brain (case 12) were stained with either primary antiserum or preadsorbed primary antiserum and then intensified, as described earlier.

Data analysis

The immunohistochemical data were visualized with a Leitz Laborlux D microscope and photographed with a Leitz Orthomat E camera. Cytoarchitectural organization of the COX-ir cell bodies was determined by localization of the intensified COX 2-ir cells on thionin-stained sections. An adjacent series of thionin-stained sections that were not stained for COX 2-ir were also used for determination of the cytoarchitecture.

Specific references to the literature are provided in cases where alternative nomenclature for the cytoarchitecture of a given region may exist.

RESULTS

Specificity of the antiserum

We used an affinity-purified antiserum raised against a unique peptide of the COX 2 sequence to ensure the specificity of the staining of COX 2-ir structures (Regier et al., 1993).

Western blot analysis (Fig. 1) revealed a COX 2-ir band (denoted by the arrow in Fig. 1) from rat cerebral cortex microsomal preparations (lane A) that comigrated with the protein band identified as COX 2 from LPS-stimulated (lane C) and unstimulated (lane D) RAW243.7 cells. This band was absent from cerebellar microsomal preparations. A second band observed in the microsomal preparations from the cerebral cortex was also observed in preparations from the cerebellum. Because we did not observe any COX 2-ir structures in the cerebellum, we have surmised that this band may represent background-stained protein or protein that does not stain in our formaldehyde-fixed tissue.

Preadsorption of the antiserum with 5 μM of DD-2 peptide completely blocked staining of both the intensified and nonintensified tissue in each region where COX 2-ir neurons were observed (Fig. 2).

COX 2-ir labeling

COX 2-ir was observed exclusively in neurons in the normal rat brain. The DAB reaction product was primarily observed in the cytoplasm of the neuronal cell body. In most cells, the proximal dendritic processes were also stained. In a few regions, such as layer 2 of the temporal cortical fields and certain amygdaloid nuclei, extensive COX 2-ir dendritic processes emanated from the cell body. No COX 2-ir nerve fibers or presumptive terminal fields were observed. The data represent a composite from all of the cases used in this study.

Telencephalon-cortex—COX 2-ir neurons were observed throughout the cerebral cortex of the rat in a unique laminar distribution in each cortical field. We have described the patterns and the morphology of these neurons in those regions described for COX 1-ir in the ovine brain by Breder et al. (1992) and also other regions that differed in modality and level of processing (e.g., TE1 vs. TE2).

Neocortex—Dense COX 2-ir labeling was observed in the primary motor cortex, Area 4 and frontal eye fields, Area 8 (Wilson, 1987; Lysakowski et al., 1989). In the primary motor cortex a dense population of small, ovoid, multipolar cells occupied the superficial aspect of laminae 2/3, whereas small pyramidal cells with prominent apical processes were observed in the deeper portion of these layers (Fig. 3B). A moderate population of large pyramidal cells was observed in the superficial aspect of lamina 5, and a sparse population of larger, intensely stained pyramidal cells was observed in the deeper portion of this layer. The morphology of the COX 2-ir neurons and pattern of staining in the frontal eye fields were similar to that observed in the primary motor cortex; however, the density of COX 2-ir cells was greater in this cortical field (Fig. 3D). The granular layer 4 is greatly diminished in this region so the COX 2-ir pyramidal cells of layer 2/3 appeared to merge with those in layer 5.

COX 2-ir neurons were observed in layers 2, 4, and 5 of the primary somatosensory cortex, Area 3b (Zilles, 1985). Moderate populations of medium-sized COX 2-ir pyramidal cells were present in layer 2, and a moderate population of small granular cells was present in layer 4 (Fig. 4B). A few large pyramidal cells were observed in the ventral portion of layer 5. In the second somatosensory cortex (Lysakowski et al., 1989), a dense population of medium-sized COX 2-ir pyramidal cells was observed in layer 2 (Fig. 4D). A small population of lightly stained, large pyramidal cells was observed in the dorsal part of layer 5.

Dense populations of small, COX 2-ir pyramidal cells were observed in layer 2 of the primary visual cortex, Area 17 (Schober and Winkelmann, 1975). A dense population of small, round granular cells was also observed in layer 4. In the secondary visual cortex, Area 18a (Schober and Winkelmann, 1975; Lysakowski et al., 19891, a very dense population of small, ovoid and medium-sized COX 2-ir cells was observed throughout laminae 2 and 3. An equally dense group of small granular cells was observed in layer 4 and the superficial aspect of layer 5. Large, lightly stained pyramidal cells were observed in the dorsal two-thirds of layer 5 of this cortical field.

A large number of densely packed COX 2-ir neurons of heterogeneous morphology was observed in layer 2 of the primary auditory cortex, Area 41 (Lysakowski et al., 1989). A group of medium- and large-sized COX 2-ir cells with extensively stained dendritic processes appeared very prominent in this layer. A few clusters of small granular cells were observed in layer 4. Small- and medium-sized pyramidal cells were diffusely distributed throughout layer 5. A very lightly stained group of COX 2-ir neurons was observed in layer 6. COX 2-ir neurons, with a similar morphology but lesser in number than those observed in area 41, were observed in layers 2, 5, and 6 of the second auditory cortex, posterior Area 22 (Lysakowski et al., 1989). Interestingly, the dendritic processes of the COX 2-ir neurons with the Golgi-like appearance in layer 2 of this region were even more extensively stained than those in area 41.

Allocortex—A dense population of COX 2-ir neurons was located in layer 3 of the infralimbic cortex (Hurley et al., 1991). This consisted of ovoid cells with one visible apical process that extended toward the medial wall of the hemisphere. This pattern of staining was readily differentiated from the adjacent prelimbic and dorsal peduncular cortices where the COX 2-ir neurons were much denser in layer 2.

COX 2-ir neurons were observed in a unique distribution in each division of the insular cortex (Cechetto and Saper, 1987). The terms anterior and posterior are used for positions in relation to the invagination of the rhinal sulcus. In the anterior portion of the dorsal granular insular cortex, a few small, ovoid cells with one apical process and a group of medium-sized pyramidal cells were observed in layer 2. A few small granular cells and large pyramidal neurons were also observed in layers 4 and 5, respectively, in this anterior region. The density of COX 2-ir cells in these laminae increased in the posterior portion of the granular insular cortex. A few medium-sized, oval, multipolar COX 2-ir neurons were observed in layer 2 of the latter region. A morphologically similar population of COX 2-ir neurons as those observed in layer 2 of the posterior granular cortex were observed throughout layer 2/3 of the dysgranular insular cortex. Although layer 4 of this field is not easily delimited in Nissl or immunohistochemical preparations, a population of small granular cells appeared to continue ventrally from those in layer 4 of the dorsal granular division. A moderate population of pyramidal cells was observed in layer 5. A dense population of small ovoid cells with one apical process was observed in laminae 2/3 of the agranular insular cortex. A small population of morphologically similar cells was observed in layer 5 of the anterior portion of this division.

The pattern of COX 2-ir neurons in the perirhinal cortex is quite complex. We have designated the perirhinal cortex as that region ventral to the TE3 and TE2 fields, dorsal to the piriform cortex (Zilles, 1985) and caudal to the insular cortex, as desitmated by Cechetto and Saper (1987). This region includes part of the posterior agranular insular cortex designated by Zilles (1985) and Lysakowski et al. (1989). We recognized dorsal and ventral divisions in the Nissl-stained coronal section of the rat brain (Fig. 5A,C,F). The dorsal and ventral divisions are not readily separated at this level, however; the pattern of Nissl stain suggests that the dorsal division occupies most of this region. The Nissl stain of the rostral perirhinal cortex in the rat is characterized by a homogeneous layer 2/3 (Fig. 5A). Cells in the superficial part of this layer are conspicuously larger than those in the deeper aspect and do not form a compact border with layer 1. Layer 5 is widest at this rostral part and less densely packed. In intermediate and caudal parts of the perirhinal cortex, both dorsal and ventral divisions are quite apparent (Fig. 5C,F). In the dorsal division, the morphology of cells in the Nissl-stained section is similar to those in the anterior part; however, they are more tightly packed, forming a discrete border with layer 1. Cells in layer 2/3 of the ventral division appear smaller on average, and a few of these spill into the overlying molecular layer. Layer 5 is not readily divided into these dorsal and ventral divisions based on the cytoarchitecture and is notably more densely packed than in the rostral portion.

A group of medium- and large-sized COX 2-ir pyramidal cells with extensively stained basilar dendritic processes was observed in the superficial half of layer 2/3 in the rostral perirhinal cortex (Fig. 5B). In caudal parts of this cortical field, the dendritic staining of these large cells increased in prominence (Fig. 5F). In the most caudal part of this region (at approximately the level of Figure 25 of Zilles, 1985), these cells were densely grouped against the border of layers 1 and 2 (Fig. 5F). The morphology and dendritic profile of these COX 2-ir neurons were quite distinct from those cells in the rostral and intermediate levels. A very dense population of small and medium-sized ovoid and pyramidal-shaped cells was also observed through-out layer 2/3 of the rostral perirhinal cortex (Fig. 5B). They were much more numerous in the dorsal than in the ventral division of intermediate and caudal levels of these layers (Fig. 5D,F). A few medium- and large-sized pyramidal cells were scattered in layer 5. These were also

preferentially distributed in the rostral part and the dorsal division of the intermediate and caudal levels of the perirhinal cortex (Fig. 5B,D,F).

COX 2-ir neurons were observed in a distinct laminar pattern in dorsal lateral, ventral lateral, and medial fields of the entorhinal cortex (Krettek and Price, 1977a). In the dorsal lateral entorhinal cortex, the densest and most intensely stained population of COX 2-ir neurons was observed in layers 2b and 3 (Fig. 6B). These were large polygonal and pyramidal-shaped cells with dendritic processes visible for a short distance from the cell body. A few lightly stained cells without stained processes were observed in layer 5. A few large polygonal COX 2-ir neurons with very extensively stained processes were observed in layer 2 and 5 of the ventral lateral entorhinal cortex (Fig. 6D). A much denser, although less intensely stained, population of medium- and large-sized polygonal COX 2-ir neurons was observed throughout layers 2,3, and 5 of this region. COX 2-ir neurons were only observed in layer 2 of the ventromedial part of the medial entorhinal cortex (Fig. 6F). These were lightly stained small and medium-sized ovoid cells with few stained processes.

Hippocampal formation—COX 2-ir neurons were discretely organized throughout the CA fields of Ammon's horn, dentate gyrus, and subicular complex (Lorente de No, 1934; Swanson et al., 1978, 1987). The densest and most intensely staining neurons in the hippocampal formation were observed in the stratum pyramidal of the CA_3 field (Figs. 7, 8A). These were characteristic pyramidal neurons with prominently stained processes projecting into the stratum radiatum. The relative number of stained apical processes decreases from the CA_{3c} to CA_{3a}, such that only the COX 2-ir cell body was visible in the latter field. The intensity of staining, but not the density, of COX 2-ir pyramidal cells appeared to decrease in a septotemporal manner. Only a few small COX 2-ir neurons were observed in the stratum pyramidal of the CAI field (Figs. 7, 8B, 9). A short nonarborizing process projected from each of these cells into the stratum radiatum. A moderate population of medium-sized ovoid neurons was observed in the stratum radiatum of the $CA_{3b,c}$ fields of the dorsal limb of the Ammon's horn (Figs. 7, 8A). Two apical processes assumed the shape of a "V" as they projected from the somata toward the stratum lacunosum-moleculare.

Dense COX 2-ir staining was also observed in the granule cell layer of the dentate gyrus (Fig. 7). Dendritic processes projected from many cells of the suprapyramidal blade into the molecular layer, whereas only a few processes were observed to emanate from the stained cells of the infrapyramidal blade. The number of cells with stained processes increased at points distal to the union of these blades. The density of the COX 2-ir granule cells was also greater in the supra- than in the infrapyramidal blade. The density of labeling in the suprapyramidal blade increased in a septotemporal direction, whereas the relative density of granule cells in the infrapyramidal blade appeared to be constant. A moderate population of medium-sized ellipsoid and triangular COX 2-ir neurons was observed in the polymorphic layer deep to the suprapyramidal blade, particularly those parts of this layer distal to the vertex of the union of the two blades (Fig. 7).

A characteristic morphology and organization of COX 2-ir neurons in the subiculum were observed in different levels of the hippocampal formation (Figs. 9, 10). A large population of medium-sized pyramidal cells was observed in the dorsal subiculum (Fig. 9).The apical dendrites of these cells were oriented perpendicular to the border of the pyramidal and plexiform layers. COX 2-ir neurons were observed in the ventral region of the subiculum only at temporal levels of the hippocampal formation (Fig. 10). At this level, the COX 2-ir neurons were observed in both dorsal and ventral portions of this structure. Unlike the subicular COX 2-ir cells in more anterior levels, the apical dendrites of these cells were not prominently stained, and the orientation of these cells appeared random. A few COX 2-ir cells were also observed within the temporal level of the postsubiculum (Fig. 10). These darkly stained, small,

ovoid cells were observed in layer 5 of this structure (Miller and Vogt, 1984;Van Groen and Wyss, 1990). A very small population of very lightly stained COX 2-ir neurons were observed in layer 2 of the parasubiculum.

Amygdala—COX 2-ir neurons were also observed in distinct portions of several nuclei of the amygdaloid complex (Figs. 11–13; DeOlmos et al., 1985;Price et al., 1987;Canteras et al., 1992). Anteriorly, a dense population of small, ovoid COX 2-ir neurons was observed in layer II of the nucleus of the lateral olfactory tract (Fig. 12). A single process projected from each of these cells toward the pial surface. This population was separated from a small group of COX 2-ir neurons in layer III by a narrow cell-sparse zone. These cells were a larger and morphologically heterogeneous. One of the most intensely staining subcortical populations of COX 2-ir neurons was observed in the ventral (McDonald and Jackson, 1987) or ventromedial division (DeOlmos et al., 1985;Turner and Herkenham, 1991) of the lateral nucleus of the amygdala (Figs. 11,13). The distribution of this group corresponds to the acetylcholine esterase (AChE)-poor region of the lateral nucleus depicted by Price et al. (1987). Most of these cells were medium-sized ovoid cells with a one stout apical process that bifurcated shortly after leaving the somata and two thin caliber processes that emerged from the opposite portion of the cell body. Intensely stained, polygonal, multipolar neurons filled the entirety of the caudal one- third of this nucleus. Many neurons of the basal magnocellular (Price et al., 1987) or anterior subdivision of the basolateral nucleus of the amygdala (Krettek and Price, 1977b;DeOlmos et al., 1985) were only very lightly stained (Figs. 11,13). Many lightly to moderately stained neurons were observed in the posterior or parvicellular (Price et al., 1987) division of the basolateral amygdaloid nucleus (Fig. 11).Several intensely stained, medium-sized ellipsoid and pyramidal neurons were observed along the lateral and ventral aspect of the anterior portions of this nucleus. A few large, intensely stained pyramidal cells were observed in the ventral basolateral amygdaloid (DeOlmos et al., 1985) or ventral endopiriform nucleus (Krettek and Price, 1977b). A moderate population of medium-sized neurons was observed in the anterior and posterior parts of the basomedial nucleus (Fig. 11). Portions of the basomedial nucleus and periamygdaloid cortex have been included in the piriform- amygdaloid area (Canteras et al., 1992). According to this system of nomenclature, medium-sized triangular neurons with three processes were densely packed in layer 2 and scattered throughout layer 3 of this structure. The cells in the posterior portion were more intensely stained. COX 2-ir neurons were observed in most of the divisions of the posteriolateral cortical amygdaloid nucleus (Fig. 11.). Most of these cells were small or medium-sized ellipsoid and pyramidal cells. In general, these cells were very densely packed in a cell layer just deep to the molecular layer. A loosely packed, less intensely stained group of COX 2-ir neurons in the deep portion of this nucleus was separated from the latter group by a thin cell-sparse zone. This stratification was most evident in the caudal medial division of this nucleus (Fig. 11). The ellipsoid cells formed a well-circumscribed oval shell around the small-celled division of this nucleus, which was conspicuously devoid of COX 2-ir neurons (Fig. 11B). A moderate population of small ellipsoid and pyramidal COX 2-ir neurons was observed within the layer 3 of the posteromedial cortical amygdaloid nucleus. This COX 2-ir cell group was circumscribed by a thin band of closely packed, unstained neuropil on their ventral aspect and a loosely packed group of neuropil on their dorsal aspect. COX 2-ir neurons were not observed in the anterior amygdaloid area or the intercalated, medial, anterior cortical, or the posterior and central amygdaloid nuclei.

Diencephalon—A dense group of heterogeneous COX 2-ir neurons was observed in the nuclei of the anteroventral region of the third ventricle (Fig. 14A,B). A very small population of large, round bipolar neurons was observed along the ventral surface of the diencephalon in the preoptic suprachiasmatic nucleus (Simerly and Swanson, 1988) extending into the ventral aspect of the vascular organ of the lamina terminalis (OVLT). A moderate population of

medium-sized fusiform cells was observed in the anteroventral and median preoptic nucleus (MnPO; Fig. 14A). These cells were uniformly oriented parallel to the border of the MnPO/OVLT and farther caudally to the wall of the third ventricle. A few of these cells were also observed in the anteroventral periventricular nucleus. At the dorsal aspect of the OVLT and third ventricle, the processes of these neurons appeared to bend in an arc along the border of the ventrally lying structures (Fig. 14B). The densest aggregation of COX 2-ir neurons outside the cortex in the rat brain occurred along the dorsal border of the OVLT in the MnPO (Fig. 14A,B). These small, heterogeneously shaped neurons were packed so densely that it was only possible to discern individual cells at high magnifications. Many of these cells were oriented perpendicular to the underlying border of the OVLT, and their processes were occasionally observed to penetrate into this circumventricular organ. This group was observed along the dorsal aspect of the third ventricle for about 500 μm caudal to its opening. A few small, round COX 2-ir cells were observed in the body of the OVLT.

A dense group of small COX 2-ir neurons was observed in the ventral, medial parvocellular part of the paraventricular nucleus of the hypothalamus (Fig. 15A,B). Neurons along the edges of this group were bipolar ellipsoid cells oriented along the border of the subnucleus. Those cells in the center of the group were polygonal and seemed randomly oriented.

A moderate population of COX 2-ir neurons was observed in the zona incerta (Fig. 16). Rostrally, a group of medium-sized fusiform neurons was observed at anterior tuberal levels of the hypothalamus, dorsal to and oriented parallel to the border of the lateral parvicellular division of the paraventricular nucleus of the hypothalamus. The density of this COX 2-ir cell group was greatest at the midtuberal region of the hypothalamus. Here the cells were observed ventral and medial to the mammillothalamic tract. At this level, these fusiform cells were slightly larger and were joined by a population of large polygonal neurons with three processes.

A very distinctive population of COX 2-ir neurons was observed in the subparafascicular nucleus of the thalamus (Fig. 17A,B). A few small polygonal neurons with three processes were observed in the rostrolateral, parvicellular portion of the nucleus (Yasui et al., 1991). A moderate population of large polygonal neurons was observed in the medial, magnocellular portion of the nucleus. In intermediate levels of this group, these large COX 2-ir neurons circumscribed the border of the nucleus in the shape of a triangle (Fig. 17A). This cell group traveled up the central gray matter in a discrete cluster that wrapped around the medial part of the parafascicular nucleus and extended dorsally into the periaqueductal gray matter (Fig. 17B). The caudalmost cells in this cell group were observed just medial to the nucleus of Darkschweitz.

Pretectum and midbrain—A moderate population of small ellipsoid COX 2-ir neurons with three processes was observed in the nucleus of the optic tract. These cells were closely aggregated in a vertical strip parallel to the lateral surface of the midbrain in the caudal part of this nucleus. In rostral sections, the cells were scattered in the ventral and lateral aspects of the nucleus among the fibers of the brachium of the superior colliculus.

A few small ovoid COX 2-ir cells were observed in the interpeduncular nucleus. These neurons were tightly clustered in the dorsal lateral subnucleus (Fig. 18; Groenewegen et al., 1986).

A small population of large multipolar COX 2-ir neurons was observed in the nucleus of the brachium of the inferior colliculus. These cells were clustered ventral to the magnocellular division of the medial geniculate body at rostral levels. Caudally, these cells formed a column, parallel to the lateral aspect of the brainstem.

Pons—A moderate population of medium-sized ellipsoid and triangular COX 2-ir neurons was observed in the pontine reticular formation. These cells were oriented parallel to the plane of pregenual fibers of the facial nerve.

A large population of COX 2-ir neurons was observed in the dorsal raphe nucleus (Fig. 19A,B). In the rostral part of this nucleus, a dense population of small, heterogeneously shaped COX 2-ir neurons were observed immediately below the cerebral aqueduct. A group of medium-sized, fusiform cells was observed between the fibers of the medial longitudinal fasciculus in the rostral ventromedial part of the dorsal raphe nucleus (Fig. 19A). A moderate population of small ovoid cells with two or three processes was observed in the caudal ventromedial part (Fig. 19B). A moderate population of small, ovoid neurons with two visible processes was observed in the lateral portion of the dorsal raphe nucleus.

Medulla and cerebellum—No COX 2-ir neurons were observed in either of the medulla or cerebellum.

DISCUSSION

This study provides detailed localization and biochemical characterization of COX 2, the inducible cyclooxygenase, in the normal rat brain. Our findings show that this enzyme is widely, yet discretely, localized throughout the brain in a distribution that is largely unique from that described for COX 1.Our results suggest that COX 2 may be involved in the integration of visceral, special, and somatosensory input and in the elaboration of the autonomic, endocrine, and behavior responses.

Technical considerations

We used an affinity-purified polyclonal antiserum raised against a carboxy terminal fragment of the murine form of COX 2 stain the rat brain. This staining was abolished by preadsorption of the antiserum, even in sections where stained tissue was later intensified with the silver–gold enhancement technique. This antiserum recognized a protein band that comigrated with the macrophage-derived COX 2 in Western blot analysis. This band was observed in microsomal preparations from parts of the brain, such as the cortex, where we observed COX 2-ir neurons, but not in the cerebellum, where no COX 2-ir structures were noted. A second band was observed in the lane containing the protein from cerebral cortex. This band was also observed in the lane containing cerebellar microsomal protein. It is therefore likely that this protein band may represent a molecular species that is not visualized as a COX 2-ir structure in paraformaldehyde-fixed tissue sections. Alternatively, it may contain protein observed as background staining.

We used a silver–gold enhancement technique to afford better visualization of the DAB reaction product. We did not detect any COX 2-ir cell groups that were not, at least to a limited extent, observed in unenhanced sections. This treatment did allow for visualization and photography at lower powers of magnification. The intensification after the preadsorption control was done as an added assurance that the cell groups visualized in this study were not artifacts of silver deposition or enhancement of cells that might artifactually appear as positively stained due to prolonged incubation in the DAB chromagen.

Anatomical considerations

Observations on the cellular distribution of COX 2—COX 2-ir was limited to the somata and proximal dendritic processes of stained neurons. We did not observe COX 2-ir axons or putative terminal fields. This cellular distribution is similar to that observed for COX 1-ir in the ovine brain (Breder et al., 1992). We therefore propose that COX may produce

prostaglandins used as either as intracellular or paracrine messengers. This capacity would also allow for communication with adjacent cells that do not have typical synapses, such as microglia, oligodendrocytes, astrocytes, or capillary endothelial cells.

Several studies have reported that cultured astrocytes have the capacity to synthesize prostaglandins, inferring the presence of some form of the cyclooxygenase enzyme (Seregi et al., 1984; Lieberman et al., 1989). Furthermore, prostaglandin D synthetase immunoreactivity has been reported in oligodendrocytes in the adult rat brain (Urade et al., 1987). To date, only one report (Tsubokura et al., 1991) on the localization of cyclooxygenase isoforms in the CNS has reported the presence of these enzymes in glia. It is possible that the expression of these enzymes in the normal CNS is below the level of detection by previously reported methods or that expression in astrocytes may be a consequence of the tissue culture preparation. Alternatively, a third glial-associated form of COX may be present in the CNS.

Comparison with the distribution of COX 1—One goal in this study was to compare the distribution of COX 1 and COX 2 systems in the CNS. Several studies have examined the distribution of the constitutive form of this enzyme, COX 1,in the brain of several different species (Breder and Saper, 1990; Tsubokura et al., 1991; Breder et al., 1992; Kawasaki et al., 1993; O'Neill and Ford-Hutchinson, 1993). The sole study performed in the rat brain involved RNA blotting analysis of the major divisions of the CNS and hybridization studies of tissue cultures (Kawasaki et al., 1993). Although their results substantiated earlier findings that COX 1 was primarily localized in neurons in the CNS (Breder et al., 1992), the anatomical resolution of blotting analysis does not allow for detailed comparison with our immunohistochemical findings.

In the study of Breder et al. (1992), three different polyclonal antisera raised against ram seminal vesical COX 1 were used to examine the distribution of COX 1 by immunohistochemistry and Western blot analysis. Although the distribution of COX 1 in the ovine brain was reported in sufficient anatomical detail, it is unclear whether those results may be compared with the present study because of potential species variability of these systems. However, given this caveat, several interesting contrasting features of the COX systems are worth noting (Table 1). In the neocortex, COX 1-ir neurons were primarily observed in layer 4, the principle lamina of modality-specific thalamocortical and feedforward corticocortical projections (cf. Coogan and Burkhalter, 1993). COX 2-ir neurons were primarily observed in layer 2, where neurons are the more likely recipient of a diffuse projection from the thalamus and polymodal sensory input from the amygdala (for review, see Saper, 1986). In the entorhinal cortex, COX 1-ir neurons were primarily observed in deep lamina, whereas COX 2-ir neurons were predominantly in layer 2b and 3. In the hippocampal formation, immunoreactive neurons of both systems are observed in the granule cell layer of the dentate gyrus. The density of cells in both systems was greater in the outer blade. These systems are contrasted in the hippocampal formation by the predominance of COX 1-ir neurons in the deep layers of the subicular complex and stratum oriens of CA_1, whereas the COX 2-ir cells were observed in the pyramidal cell layer of the CA_3 field, the subiculum proper, and superficial cell layer of the parasubiculum. Although immunoreactive neurons of both systems are found in several nuclei of the amygdala, they are both densely localized in the basomedial nucleus (DeOlmos et al., 1985). This region receives integrated, polymodal sensory input and projects to parts of the limbic telencephalon thought to be critical for the elaboration of somatomotor and visceromotor responses. These systems are contrasted in the deep amygdaloid nuclei by the predominance of stout COX 1-ir cells in the anterior part of the basolateral nucleus that bear a striking similarity in morphology to those neurons that project to limbic portions of the cortex, thalamus, and basal forebrain (McDonald, 1992). COX 2-ir neurons were primarily observed in the lateral nucleus of the amygdala. In cortical amygdaloid nuclei, COX 1-ir neurons were observed in the anterior cortical and medial nuclei of the amygdala, whereas the COX 2-ir neurons were predominantly

observed in the piriform amygdaloid area (basomedial nucleus), nucleus of the lateral olfactory tract, and posterior cortical nuclei (Canteras et al., 1992).

In the subcortical basal forebrain, neurons of both COX systems were observed in the subparafascicular nucleus and medial part of the zona incerta. In the hypothalamus, both systems are in parvocellular neurons of the paraventricular nucleus. It is unclear whether they occupy identical subnuclear distributions because these delineations have not been made in the ovine brain. Colocalization studies examining the distribution of COX 1-ir and oxytocin- or vasopressin-immunoreactive neurons would be of considerable value in this regard. Neurons of both systems were also observed in structures surrounding the anteroventral aspect of the third ventricle, including the median and anteroventral preoptic nuclei, and the vascular organ of the lamina terminalis. This relationship is particularly intriguing given the critical role of this region in the elaboration of the prostaglandin-dependent steps in the generation of the febrile response (Stitt, 1991).

In the brainstem, the caudal subcoruleus region was found to contain neurons of both systems. Colocalization studies with tyrosine hydroxylase or retrograde labeling from the spinal cord would be informative regarding the interrelationship between the COX systems and the principal, defined cell groups in this heterogeneous region. Both COX systems were also observed in different parts of some same brainstem nuclei. In the interpeduncular nucleus COX 1-ir neurons were observed in the rostral and central subnuclei, whereas COX 2-ir cells were restricted to the dorsolateral subnucleus. The development of pharmacological agents specific for each of these enzyme systems will be of great value in further differentiating their functions in the CNS.

Comparison with previous descriptions of COX 2—Two studies have reported COX 2 expression in the central nervous system. O'Neill and Ford-Hutchinson (1993) used Northern blot analysis and the reverse transcriptase-polymerase chain reaction (RT-PCR) to examine the distribution of COX 1 and COX 2 mRNA expression in several human tissues. They found that brain tissue contained the lowest level of both isoforms' mRNA. This finding is probably a reflection of the restricted regional expression of COX in the CNS (Breder et al., 1992; Yamagata et al., 1993; present study).

Yamagata et al. (1993) used in situ hybridization and immunohistochemistry to study the distribution of COX 2 mRNA and protein expression in the normal brain, and also after physiological and pharmacological stimulation. Their results were similar to those reported in the present study, particularly in the expression in neo- and allocortical fields. This study also reported expression of COX 2 mRNA in the striatum, where we observed COX 2-ir neurons in only one case (of 12 animals examined). It is not clear what striatal region or cell types were labeled in their study. Furthermore, we observed several, small to moderate populations of COX 2-ir neurons in the diencephalon and brainstem that were not reported in their study. This may be a reflection of the relatively small number of cells labeled in these nuclei, which might be difficult to separate from background labeling in the in situ hybridization technique.

Further anatomical and functional considerations

COX 2-ir neurons were observed in relatively few subcortical structures and in a characteristic laminar distribution in each field of the cortical mantle. Many of these subcortical nuclei have been reported to be involved in visceral, somatic (particularly nociceptive), or special sensory functions.

A role for COX 2 in central autonomic regulation—A prominent heterogeneous collection of COX 2-ir neurons was observed in several nuclei in the anteroventral aspect of the third ventricle (Swanson, 1987). The densest labeling in this region was in the portion of

the median preoptic nucleus that caps the anterodorsal part of the third ventricle. This nucleus receives chemosensory input from the neighboring circumventricular organs, visceral sensory information from the nucleus of the solitary tract, parabrachial nucleus, and neighboring hypothalamic nuclei, as well as input from brainstem monoaminergic nuclei involved in sensory processing related to the behavioral state (Saper and Levisohn, 1983; Swanson, 1987; Castaneyra-Perdomo et al., 1992). Physiological studies confirm that this nucleus is a critical interface for the elaboration of behavioral and visceral responses to chemosensory and visceral input used for central cardiovascular regulation (O'Neill and Brody, 1987). The presence of COX 2-ir neurons in this distribution is particularly intriguing because the median preoptic nucleus also contains the densest distribution of PGE_2 binding sites in the rat brain (Matsumura et al., 1990). Furthermore, the anteroventral region surrounding the third ventricle (including the OVLT) is the most sensitive site in the hypothalamus for the antipyretic effects of salicylate (Stitt, 1991). It would be interesting to note the effects of agents that are specific for each of the COX isoforms on the febrile response.

A distinctive group of COX 2-ir neurons was observed in the ventral medial parvocellular part of the paraventricular nucleus of the hypothalamus (Swanson and Kuypers, 1980). This region receives a particularly dense input from visceral sensory structures such as the dorsomedial nucleus of the hypothalamus (Sawchenko and Swanson, 1983) and relatively moderate inputs from autonomic regulatory nuclei in the anteroventral and medial preoptic region of the hypothalamus (Sawchenko and Swanson, 1983; Tanaka et al., 1986; Simerly and Swanson, 1988; Standaert and Saper, 1988), pons (Fulwiler and Saper, 1984), and ventrolateral medulla (Cunningham and Sawchenko, 1988). This part of the paraventricular nucleus projects to sympathetic and parasympathetic preganglionic cell groups of the medulla and spinal cord, and the dorsal horn marginal zone and central gray of discrete thoracic spinal cord segments (Swanson and McKellar, 1979). cox 2-ir neurons may therefore play a critical role in the processing of visceral sensory and noiceptive input and the generation of the ensuing autonomic response.

A role for COX 2 in special sensory function—Several regions where we observed COX 2-ir neurons are involved in highly specialized aspects of visual and auditory orientation.

A modest population of COX 2-ir neurons was observed in the nucleus of the optic tract. This nucleus receives afferent input from the contralateral retina (Berkley and Mash, 1978) and several fields of the visual cortex (Berson and Graybiel, 1980). Among the targets of its efferent projections are the superior colliculus (Edwards et al., 1979), and the part of the inferior olive giving rise to climbing fibers to the vestibulocerebellum (Simpson et al., 1979). The firing rate of most neurons in this nucleus demonstrates an azimuth toward textured objects moving in the horizontal direction. The connections and physiology of this group suggest that it is involved in relaying information on one's orientation in visual space (Simpson et al., 1979; Hoffmann and Schoppmann, 1981).

COX 2-ir neurons were also observed in several structures in the subicular complex involved in orientation. Cells in the deep layers of the postsubiculum are reciprocally connected with higher order, associational fields of the visual cortex and with the laterodorsal thalamic nucleus and is therefore considered a major visual input to the hippocampal formation and (Van Groen and Wyss, 1990). Some cells in the deep layers (4–6) of this region show a firing azimuth related to the orientation of the head in the horizontal plane (Taube et al., 1990).

A dense population of COX 2-ir neurons was also observed in the dorsal subiculum. The firing rate of many cells of this region demonstrates an azimuth in relation to visual cues in the animal's environment (Sharp and Green, 1994).

COX 2-ir neurons were also observed in a few very specialized nuclei associated with auditory processing that also receive convergent polymodal sensory input. A moderate population of large multipolar neurons was observed in the nucleus of the brachium of the inferior colliculus. Little is known about the afferent input to this specific to this nucleus. However, projections are thought to arise from the external division of the inferior colliculus and somatosensory-related cell groups such as the nonclustered neurons of the dorsal column nuclei and the lateral cervical nucleus (Berkley et al., 1986; Coleman and Clerici, 1987). Efferent projections have been studied in detail in the cat and include projections to auditory, visual, and visceral sensory structures involved in attention and orientation (Edwards et al., 1979; Van Buskirk, 1983; Kudo et al., 1984). Of particular interest are projections to parts of the auditory associative thalamus, which are thought to be involved in the assignment of emotional significance to auditory stimuli (Calford and Aitkin, 1983; Kudo et al., 1984; LeDoux et al., 1991). Single-unit recordings in this nucleus have revealed the presence of cells responding to polymodal (auditory, visual, and proprioceptive) sensory input (Blomqvist et al., 1990).

COX 2-ir neurons associated with the subparafascicular nucleus of the thalamus have a very distinctive morphology and distribution. At their rostralmost extent, the majority of these cells are components of the magnocellular division of this nucleus. Cells in this region have efferent projections to auditory association nuclei, extrapyramidal related regions, and structures associated with visual attention and orientation (Yasui et al., 1992). At intermediate levels of this group, most of the cells form a shell around the core of the medial, magnocellular part of this nucleus. This group seems to correspond to the neurons of the subparafascicular marginal zone, which contains cells that project to the spinal cord (Moriizumi and Hattori, 1992). At the caudal-most extent of this group, the COX 2-ir neurons appear identical in distribution to the group of cells Bentivoglio and Molinari (1984) described as “embracing the fasciculus retroflexus … follow[ing] its trajectory through the medial mesencephalon.” These neurons project to the inferior olive and nucleus raphe magnus. Several investigators have speculated that the magnocellular cell group is involved in the autonomic and somatic response to auditory and nociceptive stimuli (Moriizumi and Hattori, 1992; Sugiyama et al., 1992). The strong input to the inferior olive and the superior colliculus underscores the potential role of this cell group in attention and orientation toward these sensory stimuli.

COX 2-ir neurons are found in diencephalic and brain-stem regions that have been associated with processing in the visual and auditory systems. These particular regions are also the recipient of polymodal sensory input or are involved in very complex aspects (e.g., orientation) of processing this special sensory input. Physiological studies aimed at elucidating the role of prostaglandins in these systems must therefore be aimed at associational equilibrium-related aspects of these sensory systems.

A role for COX 2 in polymodal sensory integration—COX 2-ir neurons were extensively distributed in posterior and lateral portions of the deep and cortical nuclei of the amygdala. Although the inputs of these nuclei are quite diverse, they are, in general, recipient of highly convergent sensory information (Ottersen, 1982; LeDoux et al., 1991; Turner and Herkenham, 1991; Yasui et al., 1991; Canteras et al., 1992), afferents related to the state of arousal (Vertes, 1991), input about planning of viscero- and somato-motor aspects of behaviors (Price et al., 1987), and cognitive input from several polymodal association fields of the cerebral cortex (Ottersen, 1982; Canteras et al., 1992). Lesion studies by Kluver and Bucy (1939) suggested that these nuclei play a critical role in discriminating characteristics of sensory input used for the planning of behavior. This has been substantiated at the behavioral (Murray and Mishkin, 1985) and cellular (Bouma and O’Keefe, 1969) levels. Ben-Ari and Le Gal La Salle (1974) recorded from single units in the AChE-poor region of the lateral nucleus of the amygdala, where we observed a dense population of COX 2-ir neurons. Here they

observed many units with polymodal sensory responses in which the firing rates were often related to the behavioral state.

In primary sensory fields of the neocortex, COX 2-ir neurons were primarily observed in layers 2 and 4. Cell bodies in these layers (particularly layer 4) are recipient of feedforward sensory input (Coogan and Burkhalter, 1990). However, lamina in these primary sensory fields containing cells involved in ipsilateral feedforward projections (layers 3 and 5) tend not to have COX 2-ir neurons (Carvell and Simons, 1987; Coogan and Burkhalter, 1990). It is therefore likely that if the COX 2-ir neurons are the recipient of sensory information, they would relay it to other projection neurons. However, the laminae of secondary cortical fields, such as Area 18A, and the second somatosensory cortex that contain COX 2-ir neurons are the recipients of cortical feedback projections and contain cells that project back to the primary sensory cortices (Carvell and Simons, 1987; Coogan and Burkhalter, 1990).

In the allocortical fields, the laminar distribution of COX 2-ir neurons suggests that they may be innervated by the midline and intralaminar thalamic nuclei (Herkenham, 1978) and brainstem catecholaminergic and basal forebrain cholinergic nuclei (Fuxe et al., 1968; Luiten et al., 1987). These projections may be involved in cortical arousal, sensory discrimination, and regulation of the behavioral state (for review, see Saper, 1986). These superficial laminae also receive input from sensory associational cortices and polymodal sensory nuclei of the amygdaloid complex (for review, see Price et al., 1987). Projections from these layers are directed primarily toward associational fields of the cortex, the amygdala, or limbic portions of the striatum (Krettek and Price, 1977a,b; Steward and Scoville, 1978; Saper, 1982; Deacon et al., 1983; Fuller et al., 1987). The distribution of COX 2-ir neurons in these allocortical fields suggests that they are involved in complex aspects of sensory integration.

Conclusions: An inducible form of cyclooxygenase in the normal rat brain—We observed COX 2-ir neurons in parts of the CNS involved in the processing of noiceptive, visceral, and special sensory input and in the generation of a coordinated autonomic, endocrine, and behavioral response (Fig. 20). The extensive distribution of an inducible form of COX in the normal CNS may seem quite contrary. However, it is likely that the cell groups containing COX 2-ir neurons in our study represent the very limited core regions needed to acquire, integrate, and respond to sensory stimuli in the normal or basal state of the rat. In this scenario, only those animals subjected to total sensory (including visceral) deprivation would be expected not to express this enzyme. Because this state is never achieved in normal animals, a low level of expression of COX 2 must be expected. It will be of considerable interest to note the effects of different forms of sensory stimuli on the distribution of COX 2, the inducible cyclooxygenase in the CNS.

Acknowledgments

This work was supported by a grant from the National Institute of Neurological Disorders and Stroke (NS-19108), an Established Investigator Award from the American Heart Association (R.K.), the American Heart Association of Metropolitan Chicago, and the Brain Research Foundation of the University of Chicago. D.D. was supported by GM-40713. C.D.B. was supported by HD-07009.

Abbreviations

23,4,5,6	cortical laminae
3V	third ventricle
a	distal part of CA_3
AHA	anterior hypothalamic area

AMY	amygdala
aq	cerebral aqueduct
AV	anteroventral preoptic nucleus
AVPV	anteroventral periventricular region of the third ventricle
b	intermediate part of CA_3
BLa	basolateral nucleus of the amygdala, anterior part
BLp	basolateral nucleus of the amygdala, posterior part
BMp	basomedial nucleus of the amygdala, posterior part
c	proximal portion of CA_3
$CA_{1–4}$	cell fields of the Cornu Ammonis
CoA	cortical nucleus of the amygdala, anterior division
CoP1	cortical nucleus of the amygdala, posterior division, lateral part
CoPm	cortical nucleus of the amygdala, posterior division, medial part
Ctx	cortex
DG	dentate gyrus
dl	dorsal lateral part of the interpeduncular nucleus
DLEA	dorsolateral entorhinal cortex
DHA	dorsal hypothalamic area
DR	dorsal raphe nucleus
fr	fasciculus retroflexus
IP	interpeduncular nucleus
LA	lateral nucleus of the amygdala
MeA	medial nucleus of the amygdala
mlf	medial longitudinal fasciculus
MnPO	median preoptic nucleus
mp	medial parvocellular division of the paraventricular nucleus of the hypothalamus
mt	mammillothalamic tract
NBIC	nucleus of the brachium of the inferior colliculus
NLOT	nucleus of the lateral olfactory tract
NOT	nucleus of the optic tract
OVLT	vascular organ of the lamina terminalis
PAA	piriform amygdaloid area
PaS	parasubiculum
Pf	parafascicular thalamic nucleus
PoS	postsubiculum
PRF	pontine reticular formation

PVH	paraventricular nucleus of the hypothalamus
rs	rhinal sulcus
RSG	retrosplenial granular cortex
S	subiculum
sl	stratum lacunosum
so	stratum oriens
sp	stratum pyramidalis
SPF	subparafascicular nucleus
sr	stratum radiatum
TT_3	tenia tecta, dorsal division
VS	ventral subiculum
ZI	zona incerta

LITERATURE CITED

Ben-Ari Y, Le Gal LaSalle G. Lateral amygdala unit activity: II. Habituating and non-habituating neurons. Electroenceph Clin Neuro-physiol 1974;37:463–472.

Bentivoglio M, Molinari M. The interrelationships between cell groups in the caudal diencephalon of the rat to the striatum and to the medulla oblongota. Exp Brain Res 1984;54:57–65. [PubMed: 6698148]

Berkley KJ, Mash DC. Somatic sensory projections to the pretectum in the cat. Brain Res 1978;158:445–449. [PubMed: 709374]

Berkley KJ, Budell RJ, Blomqvist A, Bull M. Output systems of the dorsal column nuclei in the cat. Brain Res Rev 1986;11:199–225.

Berson DM, Graybiel AM. Some cortical and subcortical fiber projections to the accessory optic nuclei in the cat. Neuroscience 1980;5:2203–2217. [PubMed: 7465052]

Blomqvist A, Danielsson I, Norrsell U. The somatosensory intercollicular nucleus of the cats mesencephalon. J Physiol (London) 1990;429:191–203. [PubMed: 2277346]

Bouma H, O'Keefe J. Complex sensory properties of certain amygdala units in the freely moving cat. Exp Neurol 1969;23:384–398. [PubMed: 5767262]

Breder CD, Saper CB. Distribution of cyclooxygenase (PGH_2-) like immunoreactivity in the ovine central nervous system. Soc Neurosci Abstr 1990;16:496.13.

Breder CD, Smith WL, Raz A, Masferrer JL, Seibert K, Needleman P, Saper CB. The distribution and characterization of cyclooxygenase-like immunoreactivity in the ovine brain. J Comp Neurol 1992;322:409–438. [PubMed: 1517485]

Breder CD, Tsujimoto M, Terano Y, Scott D, Saper CB. The distribution and characterization of tumor necrosis factor alpha immunoreactivity in the murine central nervous system. J Comp Neurol 1993;337:543–567. [PubMed: 8288770]

Calford MB, Aitkin LM. Ascending projections to the medial geniculate body in the cat: Evidence for multiple, parallel auditory pathways through the thalamus. J Neurosci 1983;3:2365–2380. [PubMed: 6313877]

Canteras NS, Simerly RB, Swanson LW. Connections of the posterior nucleus of the amygdala. J Comp Neurol 1992;324:143–179. [PubMed: 1430327]

Carvell GE, Simons DJ. Thalamic and corticocortical connections of the second somatosensory area of the mouse. J Comp Neurol 1987;265:409–427. [PubMed: 3693613]

Castaneyra-Perdomo A, Perez-Delgado MM, Montagnese C, Coen E. Brainstem projections to the medial preoptic region containing the luteinizing hormone-releasing hormone perikarya in the rat. An immunohistochemical and retrograde transport study. Brain Res 1992;139:135–139.

Cechetto DF, Saper CB. Evidence for a viscerotopic sensory representation in the cortex and thalamus in the rat. J Comp Neurol 1987;262:27–45. [PubMed: 2442207]

Coleman JR, Clerici WJ. Sources of projections to subdivisions of the inferior colliculus in the rat. J Comp Neurol 1987;262:215–226. [PubMed: 3624552]

Coogan TA, Burkhalter A. Conserved patterns of corticocortical connections define areal hierarchy in rat visual cortex. Exp Brain Res 1990;80:49–53. [PubMed: 2358036]

Coogan TA, Burkhalter A. Hierarchical organization of area in the rat visual cortex. J Neurosci 1993;13:3749–3772. [PubMed: 7690066]

Cunningham ET, Sawchenko PE. Anatomical specificity of noradrenergic inputs to the paraventricular and supraoptic nuclei of the rat hypothalamus. J Comp Neurol 1988;274:60–76. [PubMed: 2458397]

Deacon TW, Eichenbaum H, Rosenberg P, Eckman KW. Afferent connections of the perirhinal cortex in the rat. J Comp Neurol 1983;220:168–190. [PubMed: 6643724]

DeOlmos, J.; Alheid, GF.; Beltramino, C. Amygdala. In: Paxinos, G., editor. The Rat Central Nervous System. Sydney: Academic Press; 1985. p. 223-334.

Dewitt DL, Meade EA. Serum and glucocorticoid regulation of gene transcription and expression of the prostaglandin H synthase-1 and prostaglandin H synthase-2 isozymes. Arch Biochem Biophys 1993;306:94–102. [PubMed: 8215426]

Dewitt DL, Smith WL. Cloning of sheep and mouse prostaglandin endoperoxide synthases. Methods in Enzymology 1990;187:469–479. [PubMed: 2122186]

Edwards SB, Ginsburgh CL, Henkel CK, Stein BE. Sources of subcortical projections to the superior colliculus in the cat. J Comp Neurol 1979;184:309–330. [PubMed: 762286]

Fuller TA, Russchen FT, Price JL. Sources of presumptive glutamergic/aspartergic afferents to the rat ventral striatopallidal region. J Comp Neurol 1987;258:317–338. [PubMed: 2884240]

Fulwiler CE, Saper CB. Subnuclear organization of the efferent connections of the parabrachial nucleus in the rat. Brain Res Rev 1984;7:229–259.

Fuxe K, Hamberger B, Hokfelt T. Distribution of noradrenaline nerve terminals in cortical areas of the rat. Brain Res 1968;8:125–131. [PubMed: 5650798]

Groenewegen HJ, Ahlenius S, Haber SN, Kowall NW, Nauta WJH. Cytoarchitecture, fiber connections, and some histochemical aspects of the interpeduncular nucleus in the rat. J Comp Neurol 1986;249:65–102. [PubMed: 2426312]

Hayaishi O. Molecular mechanisms of sleep-wake regulation—Roles of prostaglandin-D_2 and prostaglandin-E_2. FASEB J 1991;5:2575–2581. [PubMed: 1907936]

Hedqvist P. Basic mechanisms of prostaglandin action on autonomic neurotransmission. Annu Rev Pharmacol Toxicol 1977;17:259–279. [PubMed: 194531]

Herkenham M. The connections of the nucleus reuniens thalami: Evidence for a direct thalamo-hippocampal pathway in the rat. Brain Res 1978;177:589–610.

Hoffmann KP, Schoppmann A. Quantitative analysis of the direction-specific response of neurons. Exp Brain Res 1981;42:146–157. [PubMed: 7262211]

Horiguchi S, Ueno R, Hyodo M, Hayaishi O. Alteration in nociception after intracisternal administration of prostaglandin D_2, E_2 or F_{2a} to conscious mice. Eur J Pharmacol 1986;122:173–179. [PubMed: 3458588]

Hurley KM, Herbert H, Moga MM, Saper CB. The efferent connections of the infralimbic cortex in the rat. J Comp Neurol 1991;308:249–276. [PubMed: 1716270]

Kawasaki M, Yoshihara Y, Yamaji M, Watanabe Y. Expression of prostaglandin endoperoxide synthase in rat brain. Molec Brain Res 1993;19:39–46. [PubMed: 8361344]

Kluver H, Bucy PC. Preliminary analysis of the functions of the temporal lobe in monkeys. Arch Neurol Psych 1939;42:979–1000.

Krettek JE, Price JL. Projections from the amygdaloid complex and adjacent olfactory structures to the entorhinal cortex and to the subiculum in the rat and cat. J Comp Neurol 1977a;172:723–752. [PubMed: 838896]

Krettek JE, Price JL. Projections from the amygdaloid complex to the cerebral cortex and thalamus in the rat and cat. J Comp Neurol 1977b;172:687–722. [PubMed: 838895]

Kudo M, Tashiro T, Higo S, Matsuyama T, Kawamura S. Ascending projections from the nucleus of the brachium of the inferior colliculus in the cat. Exp Brain Res 1984;54:203–211. [PubMed: 6327347]

LeDoux JE, Farb CR, Romanski LM. Overlapping projections to the amygdala and striatum from auditory processing areas of the thalamus and cortex. Neurosci Lett 1991;134:139–144. [PubMed: 1815147]

Lieberman AP, Pitha PM, Shin HS, Shin ML. Production of tumor necrosis factor an other cytokines by astrocytes stimulated with lipopolysaccharide or a neurotropic virus. Proc Natl Acad Sci USA 1989;86:6348–6352. [PubMed: 2474832]

Loewy, AD. Central autonomic pathways. In: Loewy, AD.; Spyer, KM., editors. Central Regulation of Autonomic Functions. New York: Oxford University Press; 1990. p. 88-103.

Lorente de No R. Studies on the structure of the cerebral cortex: II. Continuation of the study of the ammonic system. J für Psych Neurol 1934;46:113–177.

Luiten PGM, Gaykema RPA, Traber J, Spencer DG. Cortical projection patterns of magnocellular basal nucleus subdivisions as revealed by anterogradely transported *Phaseolus vulgaris* leucoagglutinin. Brain Res 1987;413:229–250. [PubMed: 3300852]

Lysakowski A, Wainer BH, Bruce G, Hersch LB. An atlas of the regional and laminar distribution of choline acetyltransferase immunoreactivity in the rat cerebral cortex. Neuroscience 1989;28:291–336. [PubMed: 2646551]

Matsumura K, Watanabe Y, Onoe H, Hayaishi O. High density of prostaglandin-E2 binding sites in the anterior wall of the 3rd ventricle—A possible site of its hyperthermic action. Brain Res 1990;533:147–151. [PubMed: 1964828]

McDonald AJ. Projection neurons of the basolateral amygdala—A correlative golgi and retrograde tract tracing study. Brain Res Bull 1992;28:179–185. [PubMed: 1375860]

McDonald AJ, Jackson TR. Amygdaloid connections with posterior insular and temporal cortical areas in the rat. J Comp Neurol 1987;262:59–77. [PubMed: 2442208]

Miller MW, Vogt BA. Direct connections of rat visual with sensory, motor and association cortices. J Comp Neurol 1984;226:184–202. [PubMed: 6736299]

Moriizumi T, Hattori T. Anatomical and functional compartmentalization of the subparafascicular thalamic nucleus in the rat. Exp Brain Res 1992;90:175–179. [PubMed: 1381685]

Murray EA, Mishkin M. Amygdalectomy impairs crossmodal association in monkeys. Science 1985;228:604–606. [PubMed: 3983648]

O'Neill GP, Ford-Hutchinson AW. Expression of mRNA for cyclooxygenase-1 and cyclooxygenase-2 in human tissues. FEBS Lett 1993;2:156–160.

O'Neill TP, Brody MJ. Role for the median preoptic nucleus in centrally evoked pressor responses. Am J Physiol 1987;252:R1165–R1172. [PubMed: 3591987]

Ojeda S, Negro-Vilar A, McCann SM. Evidence for involvement of alpha adrenergic receptors in norepinephrine induced PGE2 and luteinizing hormone releasing hormone from the median eminence. Endocrinology 1982;110:409–412. [PubMed: 6276133]

Ottersen OP. Connections ofthe amygdala of the rat. IV. Corticoamygaloid and intra-amygdaloid connections as studies with axonal transport of horseradish peroxidase. J Comp Neurol 1982;205:30–48. [PubMed: 7068948]

Price, JL.; Russchen, FT.; Amaral, DG. The limbic region. II: The amygdaloid complex. In: Bjorklund, A.; Hokfelt, T.; Swanson, LW., editors. Handbook of Chemical Neuroanatomy, vol. 5: Integrated Systems of the CNS, part 1: Hypothalamus, Hippocampus, Amygdala, Retina. New York: Elsevier; 1987. p. 279-388.

Reiger MK, DeWitt DL, Schindler MS, Smith WS. Subcellular localization of prostaglandin endoperoxide synthase-2 in murine 3T3 cells. Arch Bioch Biophys 1993;301:439–444.

Saper CB. Convergence of autonomic and limbic connections in the insular cortex of the rat. J Comp Neurol 1982;210:163–173. [PubMed: 7130477]

Saper, CB. Diffuse cortical projection systems: Anatomical organization and role in cortical function. In: Plum, F., editor. Handbook of Physiology, vol. V: The Nervous System. Bethesda, MD: American Physiological Society; 1986. p. 169-210.

Saper CB, Levisohn D. Afferent connections of the median preoptic nucleus in the rat: Anatomical evidence for a cardiovascular integrative mechanism in the anteroventral third ventricular (AV3V) region. Brain Res 1983;288:21–31. [PubMed: 6198025]

Sawchenko PE, Swanson LW. The organization of forebrain afferents to the paraventricular and supraoptic nuclei of the rat. J Comp Neurol 1983;218:121–144. [PubMed: 6886068]

Schober W, Winkelmann E. Der visuelle Kortex der ratte cytoarchitektonik and stereotaktische parameter. Z Mikrosk Anat Forsch (Leipzig) 1975;89:431–446.

Seregi A, Keller M, Jackisch R, Hertting G. Comparison of the prostanoid synthesizing capacity in homogenates from primary neuronal and astroglial cell lines. Biochem Biophys Res Comm 1984;33:3315–3318.

Sharp PE, Green C. Spatial correlates of firing patterns of single cells in the subiculum of the freely moving rat. J Neurosci 1994;14:2339–2356. [PubMed: 8158272]

Simerly RB, Swanson LW. Projections of the medial preoptic nucleus: A *Phaseolus vulgaris* leucoagglutinin anterograde tract-tracing study in the rat. J Comp Neurol 1988;270:209–242. [PubMed: 3259955]

Simpson, JI.; Soodak, RE.; Hess, RG. The accessory optic system and its relation to the vestibulocerebellum. In: Granit, R.; Pompeiano, O., editors. Progress in Brain Research, vol. 50: Reflex Control of Posture and Movement. Amsterdam: Elsevier; 1979. p. 715-724.

Smith WL, Marnett LJ, Dewitt D. Prostaglandin and throm-boxane biosynthesis. Pharmacol Ther 1991;49:153–179. [PubMed: 1905023]

Standaert DG, Saper CB. Origin of the atriopeptin-like immunoreactive innervation of the paraventricular nucleus of the hypothalamus. J Neurosci 1988;8:1940–1950. [PubMed: 2968443]

Steward O, Scoville SA. Cells of origin of entorhinal cortical afferents to the hippocampus and fascia dentata of the rat. J Comp Neurol 1978;169:347–370. [PubMed: 972204]

Stitt JT. Differential sensitivity in the sites of fever production by prostaglandin-E1 within the hypothalamus of the rat. J Physiol (London) 1991;432:99–110. [PubMed: 1886074]

Sugiyama KT, Ryu H, Uemura K. Identification of nociceptive neurons in the medial thalamus: Morphological studies of nociceptive neurons with intracellular injection of horseradish peroxidase. Brain Res 1992;586:36–43. [PubMed: 1380880]

Swanson, LW. The hypothalamus. In: Bjorklund, A.; Hokfelt, T.; Swanson, LW., editors. Handbook of Chemical Neuroanatomy, vol. 5: Integrated Systems of the CNS, part 1: Hypothalamus, Hippocampus, Amygdala, Retina. New York: Elsevier; 1987. p. 1-124.

Swanson LW, Kuypers HGJM. The paraventricular nucleus of the hypothalamus: Cytoarchitectonic subdivisions and organization of projections to the pituitary, dorsal vagal complex and spinal cord as demonstrated by retrograde double-labeling methods. J Comp Neurol 1980;194:555–570. [PubMed: 7451682]

Swanson LW, McKellar S. The distribution of oxytocin and neurophysin-stained fibers in the spinal card if the rat and monkey. J Comp Neurol 1979;188:87–106. [PubMed: 115910]

Swanson LW, Wyss JM, Cowan WM. An autoradiographic study of the organization of intrahippocampal association pathways in the rat. J Comp Neurol 1978;181:681–716. [PubMed: 690280]

Swanson, LW.; Kohler, C.; Bjorklund, A. The limbic region. I: The septohippocampal system. In: Bjorklund, A.; Hokfelt, T.; Swanson, LW., editors. Handbook of Chemical Neuroanatomy, vol. 5: Integrated Systems of the CNS, part 1: Hypothalamus, Hippocampus, Amygdala, Retina. Amsterdam: Elsevier; 1987. p. 125-277.

Tanaka J, Kaba H, Saito H, Seto K. Lateral hypothalamic area stimulation excites neurons in the region of the subfornical organ with efferent projections to the hypothalamic paraventricular nucleus in the rat. Brain Res 1986;379:200–203. [PubMed: 3742216]

Taube JS, Muller RU, Ranck JB Jr. Head direction cells recorded from the postsubiculum in freely moving rats. I. Description and quantitative analysis. J Neurosci 1990;10:420–435. [PubMed: 2303851]

Tork I, Leventhal AG, Stone J. Brain stem afferents to visual cortical areas 17, 18 and 19 in the cat, demonstrated by horseradish peroxidase. Neurosci Lett 1979;11:247–252. [PubMed: 514536]

Tsubokura S, Watanabe Y, Ehara H, Imamura K, Sugimoto O, Kagamiyama H, Yamamoto S, Hayaishi O. Localization of prostaglandin endoperoxide synthase in neurons and glia in monkey brain. Brain Res 1991;543:15–24. [PubMed: 1905180]

Turner BH, Herkenham M. Thalamoamygdaloid projections in the rat—A test of the amygdala's role in sensory processing. J Comp Neurol 1991;313:295–325. [PubMed: 1765584]

Urade Y, Fujimiya N, Kaneko T, Konishi A, Mizuno N, Hayaishi O. Postnatal changes in the localization of prostaglandin D synthetase from neurons to oligodendrocytes in the rat brain. J Biol Chem 1987;262:15132–15136. [PubMed: 3117794]

Van Buskirk RL. Subcortical auditory and somatosensory afferents to hamster superior colliculus. Brain Res Bull 1983;10:583–587. [PubMed: 6871733]

Van Groen T, Wyss JM. The postsubicular cortex in the rat—Characterization of the 4th Region of the subicular cortex and its connections. Brain Res 1990;529:165–177. [PubMed: 1704281]

Vertes RP. A PHA-L analysis of ascending projections of the dorsal raphe nucleus in the rat. J Comp Neurol 1991;313:643–668. [PubMed: 1783685]

Wilson CJ. Morphology and synaptic connections of crossed corticostriatal neurons in the rat. J Comp Neurol 1987;263:567–580. [PubMed: 2822779]

Xie WL, Chipman JG, Robertson DL, Erikson RL, Simmons DL. Expression of a mitogen-responsive gene encoding prostaglandin synthase is regulated by messenger RNA splicing. Proc Natl Acad Sci USA 1991;88:2692–2696. [PubMed: 1849272]

Yamagata K, Andreasson KI, Kaufmann WE, Barnes CA, Worley PF. Expression of a mitogen-inducible cyclooxygenase in brain neurons: Regulation by synaptic activity and glucocorticoids. Neuron 1993;11:371–386. [PubMed: 8352945]

Yasui Y, Saper CB, Cechetto DF. Calcitonin gene-related peptide (CGRP) immunoreactive projections from the thalamus to the striatum and amygdala in the rat. J Comp Neurol 1991;308:293–310. [PubMed: 1890240]

Yasui Y, Nakano K, Mizuno N. Descending projections from the subparafascicular thalamic nucleus to the lower brainstem in the rat. Exp Brain Res 1992;90:508–518. [PubMed: 1385199]

Zilles, K. The Cortex of the Rat. Heidelberg: Springer-Verlag; 1985.

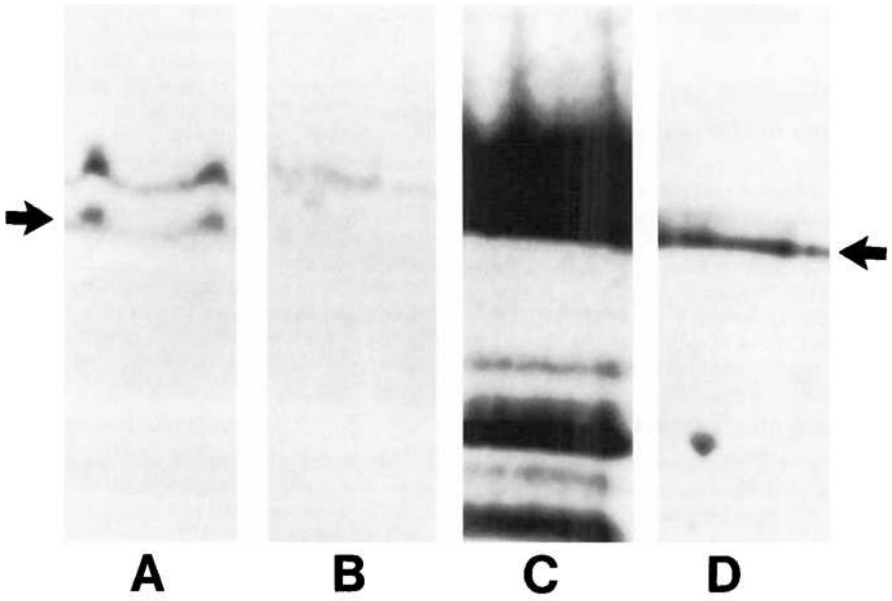

Fig. 1.

Western blot analysis of cyclooxygenase 2-like immunoreactivity (COX 2-ir). Lanes: **A:** rat brain cerebral cortex; **B:** rat brain cerebellum; **C:** lipopolysaccharide (LPS)-stimulated RAW 243.7 cells; and **D:** unstimulated RAW 243.7 cells. The arrows denote the position of the COX 2 protein.

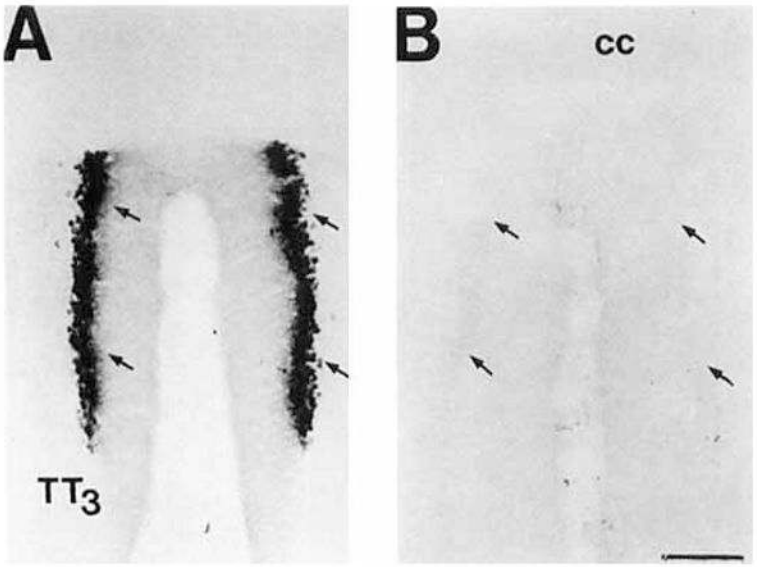

Fig. 2.

A: Brightfield photomicrograph of COX 2-ir neurons in the granular cell layer of the dorsal, TT_3, region of the tenia tecta. **B:** The adjacent section stained with the primary COX 2-ir antiserum pread- sorbed with the DD-2 peptide. Note the lack of staining despite intensification of the control material. The arrows denote the position of the granular cell layer of this division. Scale bar = 150 μm.

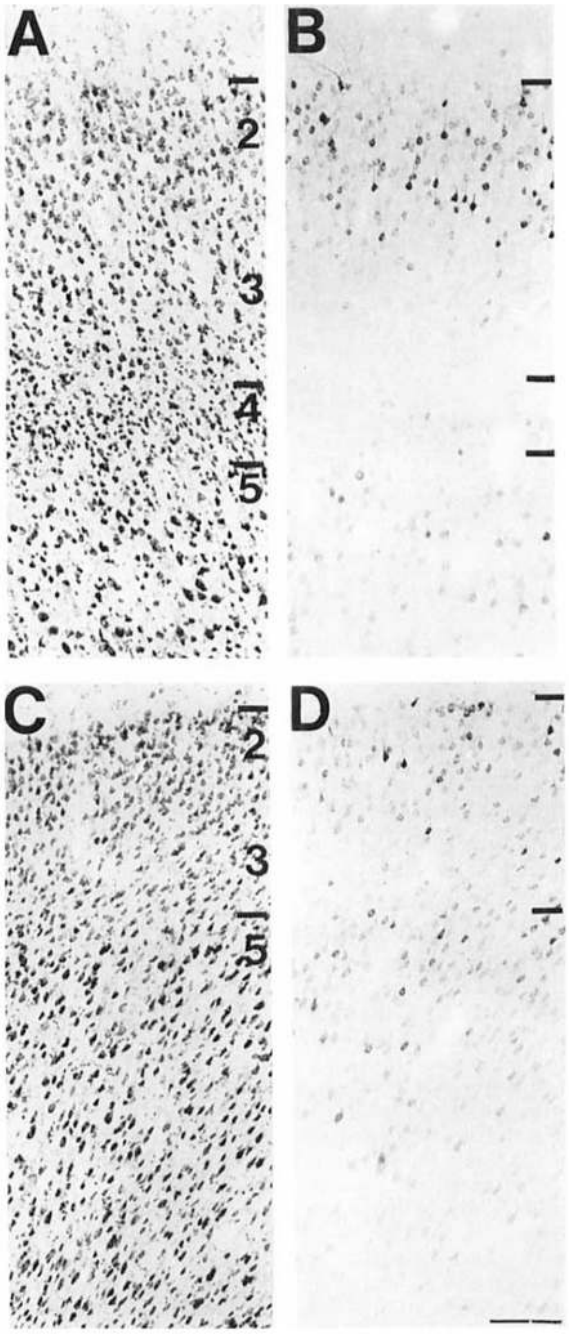

Fig. 3.

A series of brightfield photomicrographs demonstrate the laminar organization of COX 2-ir neurons in motor fields of the cortex (**A,C**). Laminae are indicated on the adjacent Nissl-stained sections (**B,D**). A,B: Primary motor cortex. C,D: Frontal eye field. Scale bar = 100 μm.

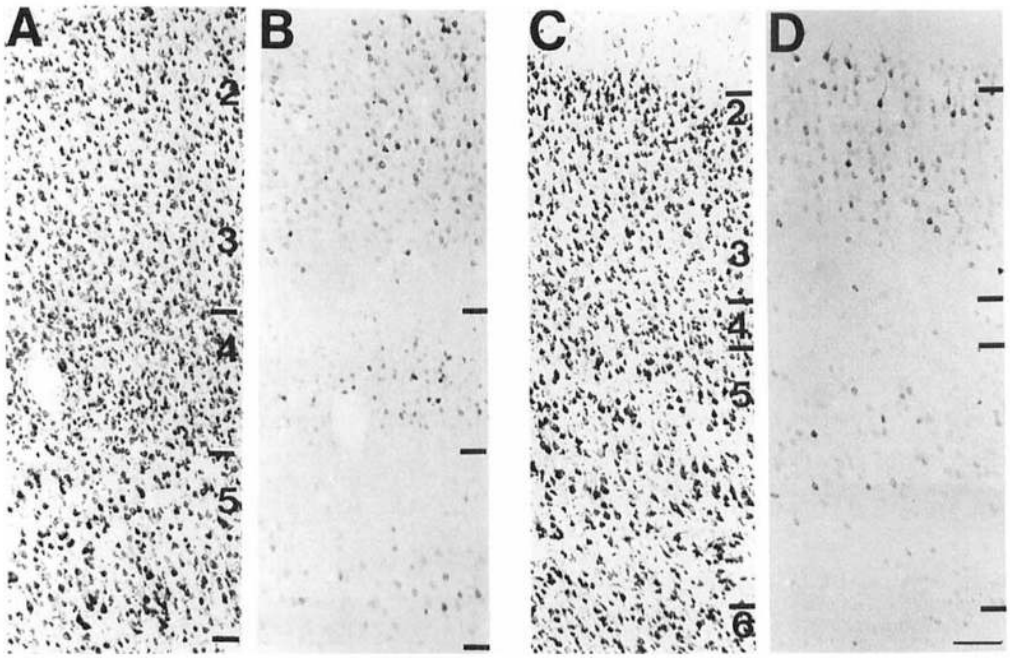

Fig. 4.

A series of brightfield photomicrographs demonstrate the laminar organization of COX 2-ir neurons in somatosensory fields of the cortex (**A,C**). Laminae are indicated on the adjacent Nissl-stained sections (**B,D**). A,B: Primary somatosensory cortex. C,D: Secondary somatosensory cortex. Scale bar = 100 μm

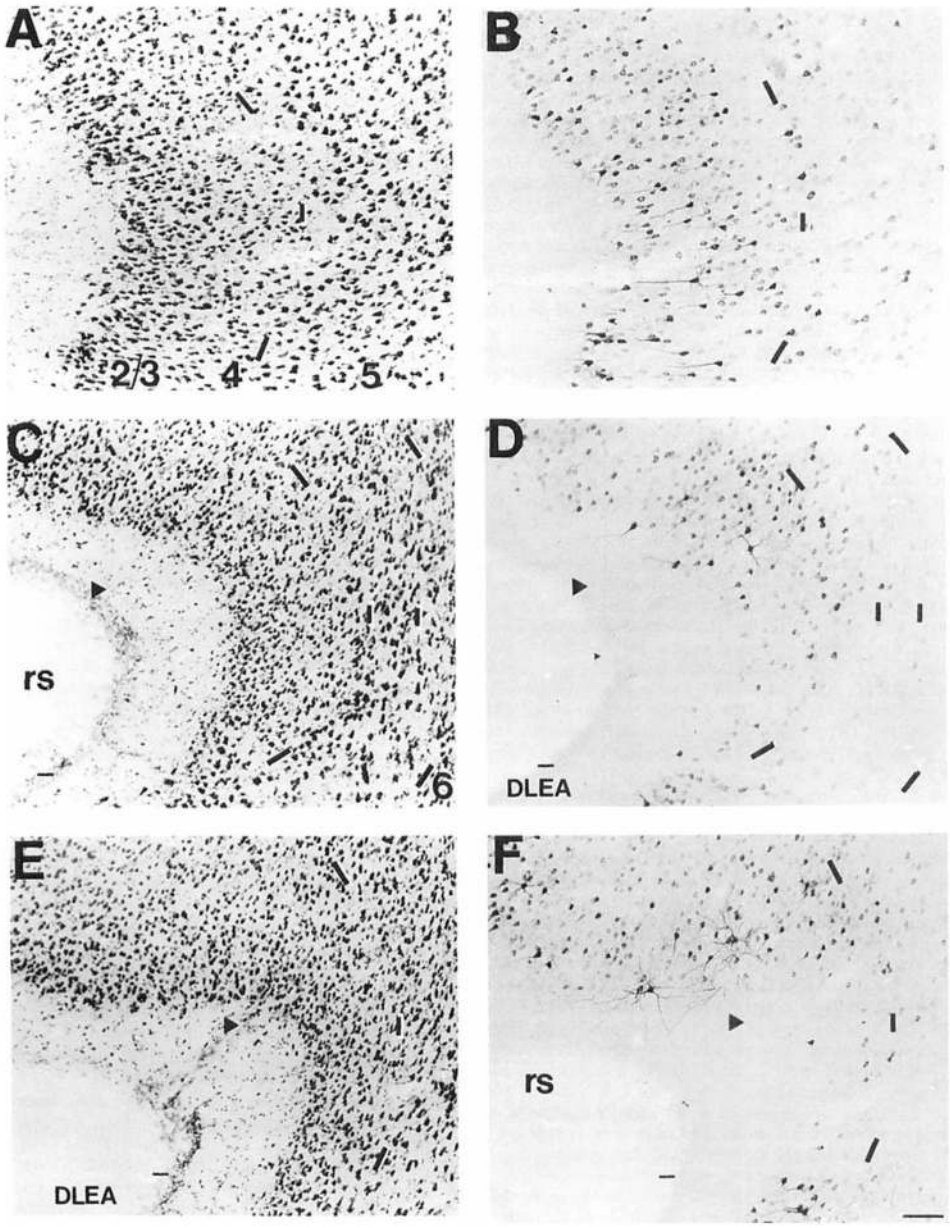

Fig. 5.

A series of brightfield photomicrographs demonstrate the laminar organization of COX 2-ir neurons in several levels of the perirhinal cortex (**A,C,E**). Photomicrographs are oriented in the normal transverse view. The arrowheads denote the deepest portion of the invagination of the rhinal sulcus, which we have taken as the division of the dorsal and ventral portions of this cortical field. Laminae are indicated in the adjacent Nissl-stained sections (**B,D,F**). A,B: Rostral perirhinal cortex, approximately at the level of Figure 19 of Zilles (1985). C,D: Intermediate perirhinal cortex, approximately at the level of Figure 23 of Zilles (1985). E,F: Caudal perirhinal cortex, approximately at the level of Figure 25 of Zilles (1985). Dashes in A, C, and E correspond to the lamina boundaries in B, D, and F. Scale bar = 100 μm.

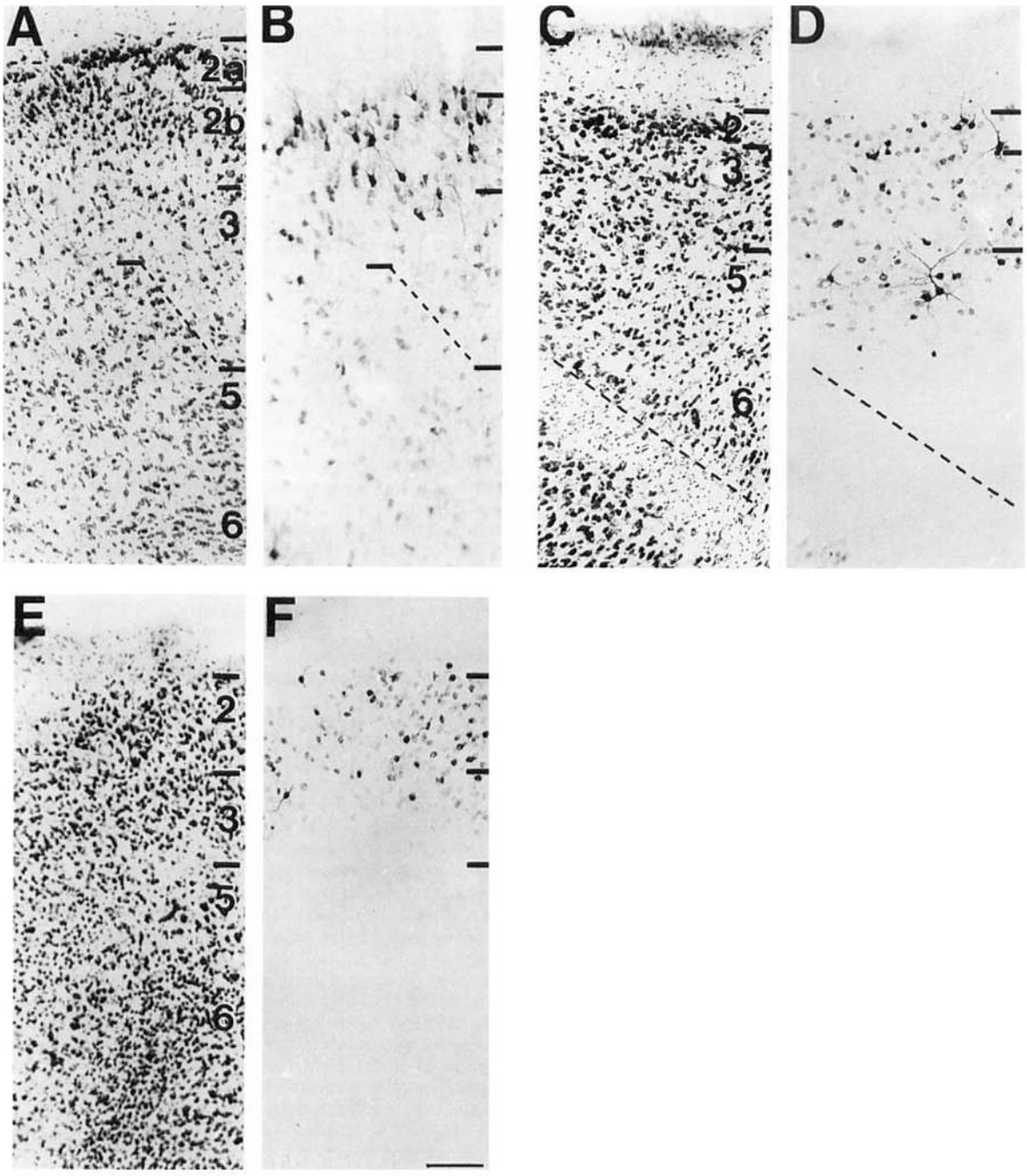

Fig. 6.

A series of brightfield photomicrographs demonstrate the laminar organization of COX 2-ir neurons in different fields of the entorhinal cortex (**A,C,E**). The dorsal aspect (closest to the rhinal sulcus) of each section is positioned on the right side. Laminae are indicated in the adjacent Nissl-stained sections (**B,D,F**) and are further delineated in certain sections by the use of dashed lines. A,B: Lateral entorhinal cortex. C,D: Ventrolateral entorhinal cortex. E,F: Medial entorhinal cortex. Scale bar = 100 μm.

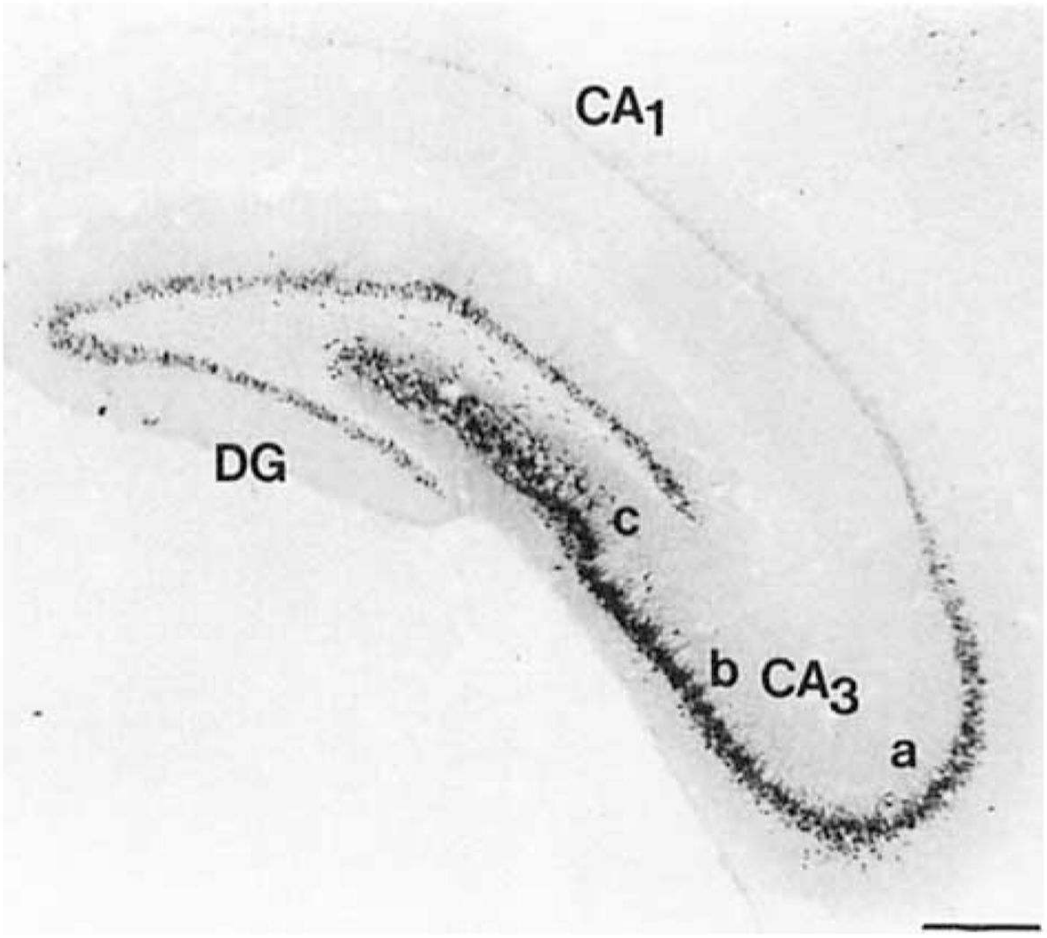

Fig. 7.
A low-power brightfield photomicrograph of COX 2-ir neurons in the dorsal hippocampal formation. Scale bar = 300 μm.

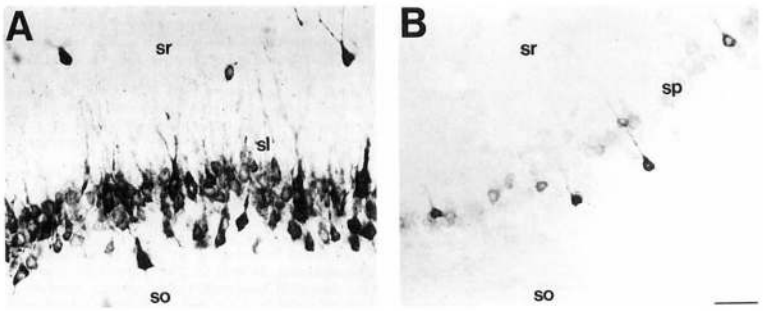

Fig. 8.

A pair of brightfield photomicrographs show COX 2-ir neurons in the cell fields of the Cornu ammonis. **A:** COX 2-ir neurons in the C& field. Note the dense staining of cells in the stratum pyramidalis and sparse population of COX 2-ir cells in the stratum radiatum. **B**: A sparse population of COX 2-ir neurons were observed in the stratum pyramidalis of the CA_1 field. Scale bar = 50 μm.

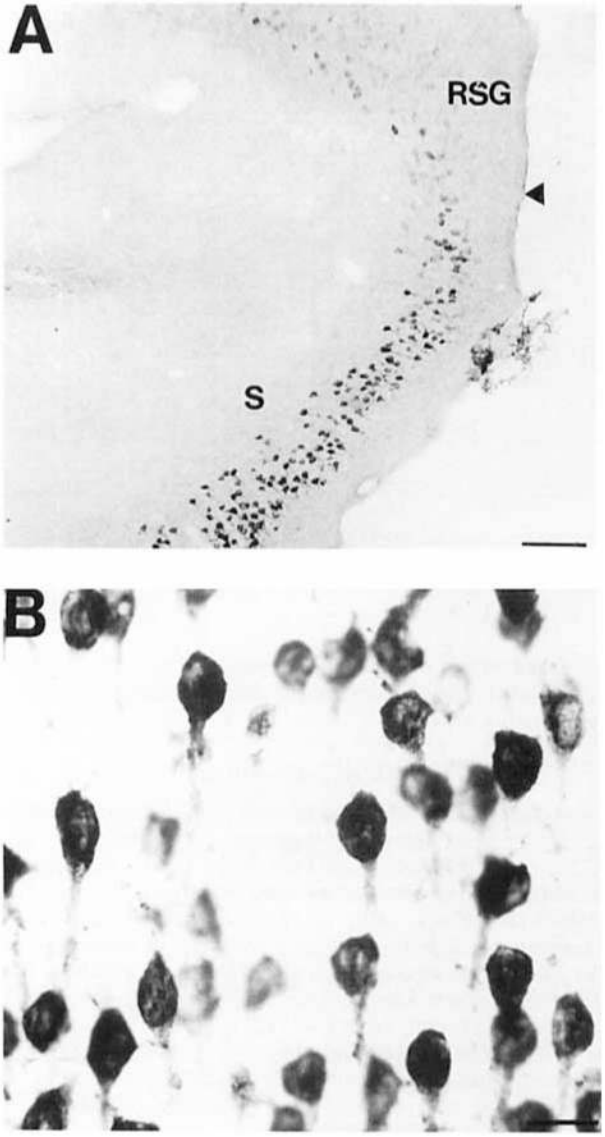

Fig. 9.

A pair of brightfield photomicrographs depict COX 2-ir neurons in the dorsal subiculum. **A:** A low-power photomicrograph of COX 2-ir neurons in the subiculum at the level of the splenium of the corpus callosum. The arrowhead denotes the border with the retrosplenial granular cortex. **B:** A high-power photomicrograph of the COX 2-ir neurons in the dorsal subiculum. Note the uniformity of the ventral processes projecting from these neurons. Scale bars = 100 μm in A, 20 μm in B.

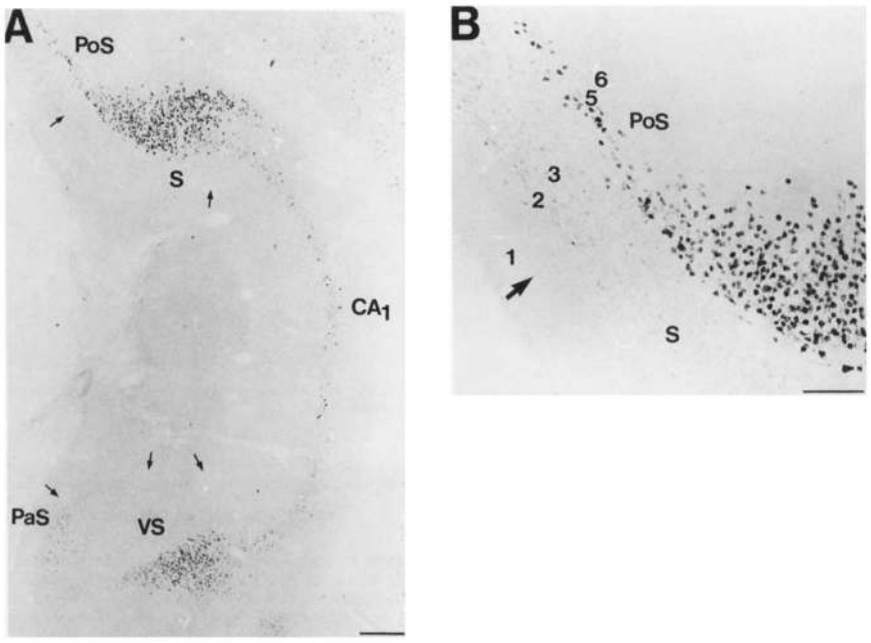

Fig. 10.

A pair of brightfield photomicrographs depict the COX 2-ir neurons in the temporal portion of the hippocampal formation. **A:** A low-power photomicrograph depicts COX 2-ir neurons in the dorsal and ventral portions of the subiculum, postsubiculum, and stratum pyramidal of CA_1. The arrows delineate regional boundaries in the subicular region of the hippocampal formation. **B:** High-power photomicrograph depicts the COX 2-ir neurons in the dorsal division of the temporal part of the subiculum and the laminar organization of the COX 2-ir neurons in the postsubiculum. The numbers denote the laminae in the postsubiculum and the arrow marks its border with the dorsal subiculum. Scale bars = 300 μm in A, 150 μm in B.

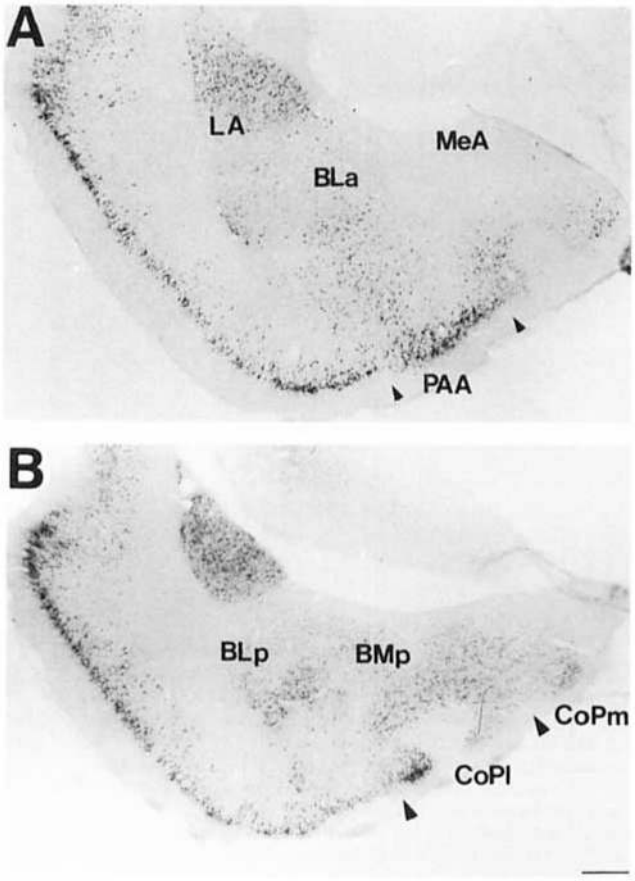

Fig. 11.
A pair of low-power brightfield photomicrographs depict the COX 2-ir neurons in the (**A**) middle level of the amygdala and (**B**) posterior level of the amygdala. Scale bar = 300 μm.

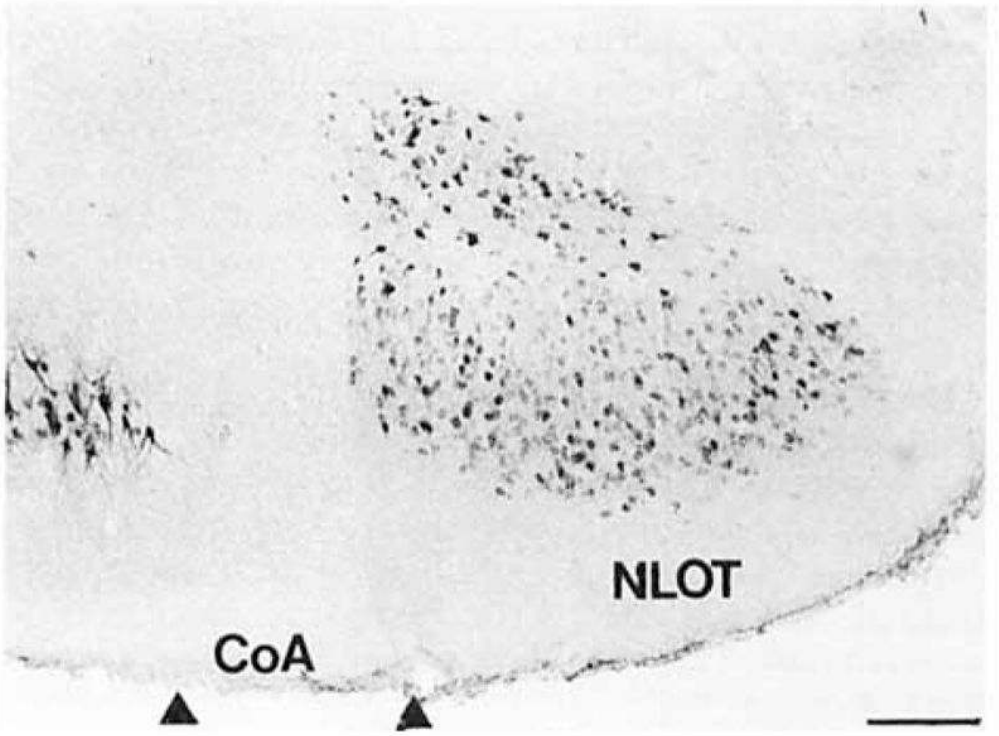

Fig. 12.
A hrightfield photomicrograph depicts COX 2-ir neurons in the nucleus of the lateral olfactory tract. Scale bar = 200 μm.

Fig. 13.
A high-power photomicrograph depicts COX 2-ir neurons in the lateral nucleus of the amygdala. Scale bar = 30 μm.

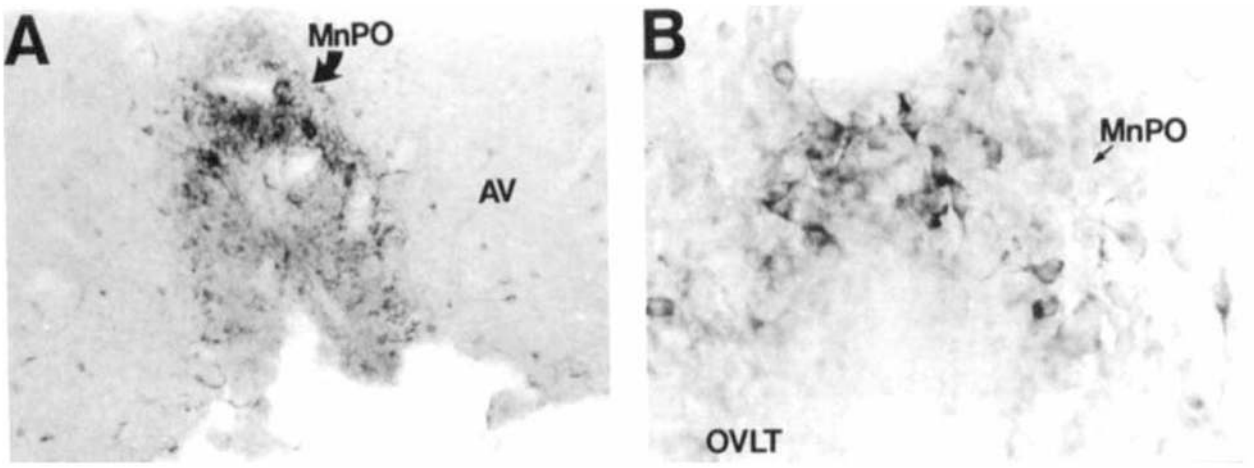

Fig. 14.

A series of brightfield photomicrographs depict COX 2-ir neurons in the anteroventral region of the third ventricle. **A:** A low-power photomicrograph depicts COX 2-ir neurons in the rostra1 anteroventral region of the third ventricle. Dense aggregates of these neurons were observed in the median preoptic nucleus and vascular organ of the lamina terminalis and less densely in the anteroventral periventricular nucleus. **B:** A high-power photomicrograph depicts COX 2-ir neurons in the dorsal aspect of the third ventricle in the median preoptic nucleus. Scale bars = 100 μm in A, 30 μm in B.

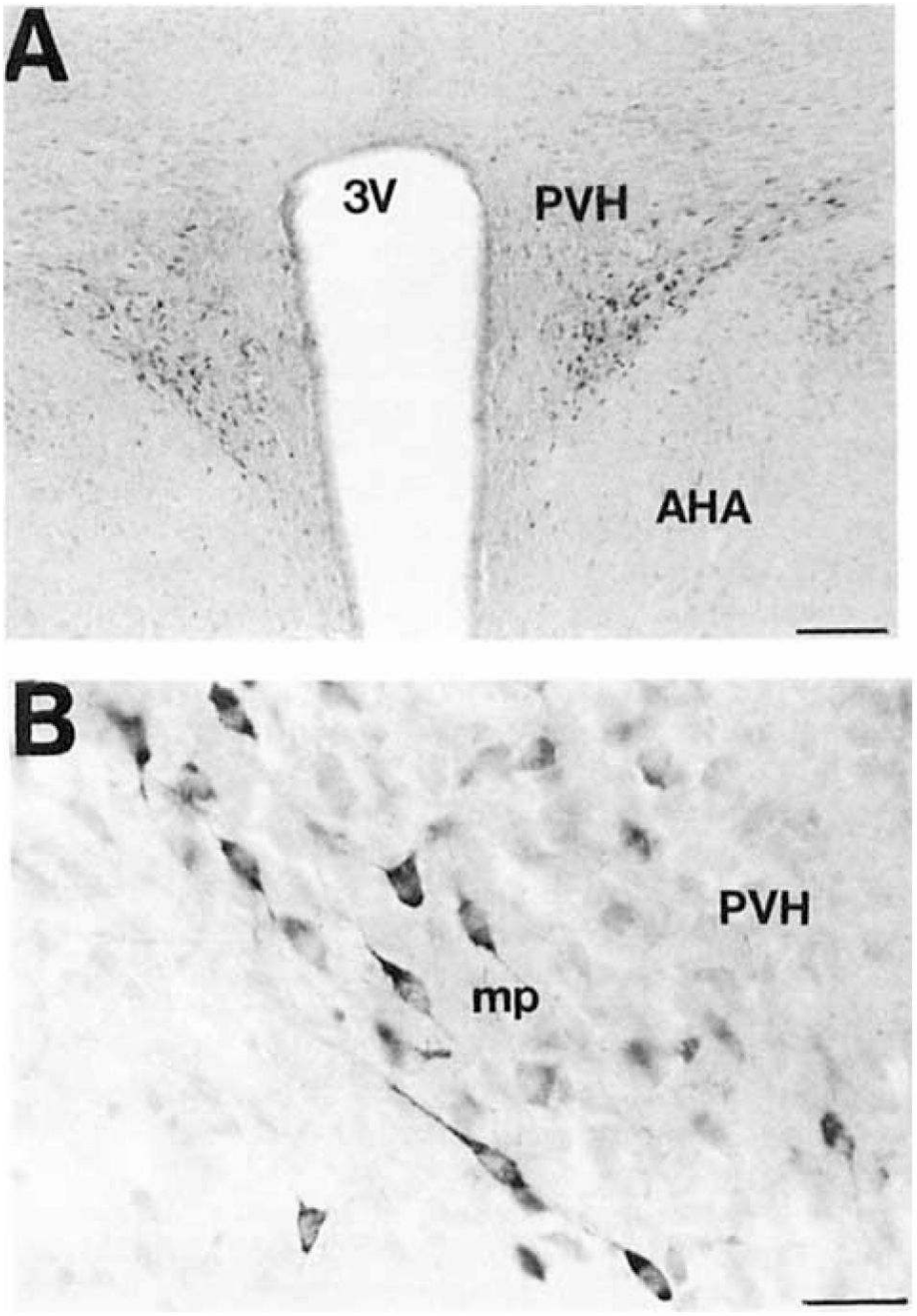

Fig. 15.

A pair of brightfield photomicrographs depict COX 2-ir neurons in the paraventricular nucleus of the hypothalamus. **A:** A low-power photomicrograph depicts the COX 2-ir neurons in the ventral portion of the medial parvocellular subnucleus of the paraventricular nucleus of the hypothalamus. **B:** A high-power photomicrograph depicts the COX 2-ir neurons in this division. Scale bars = 150 μm in A, 30 μm in B.

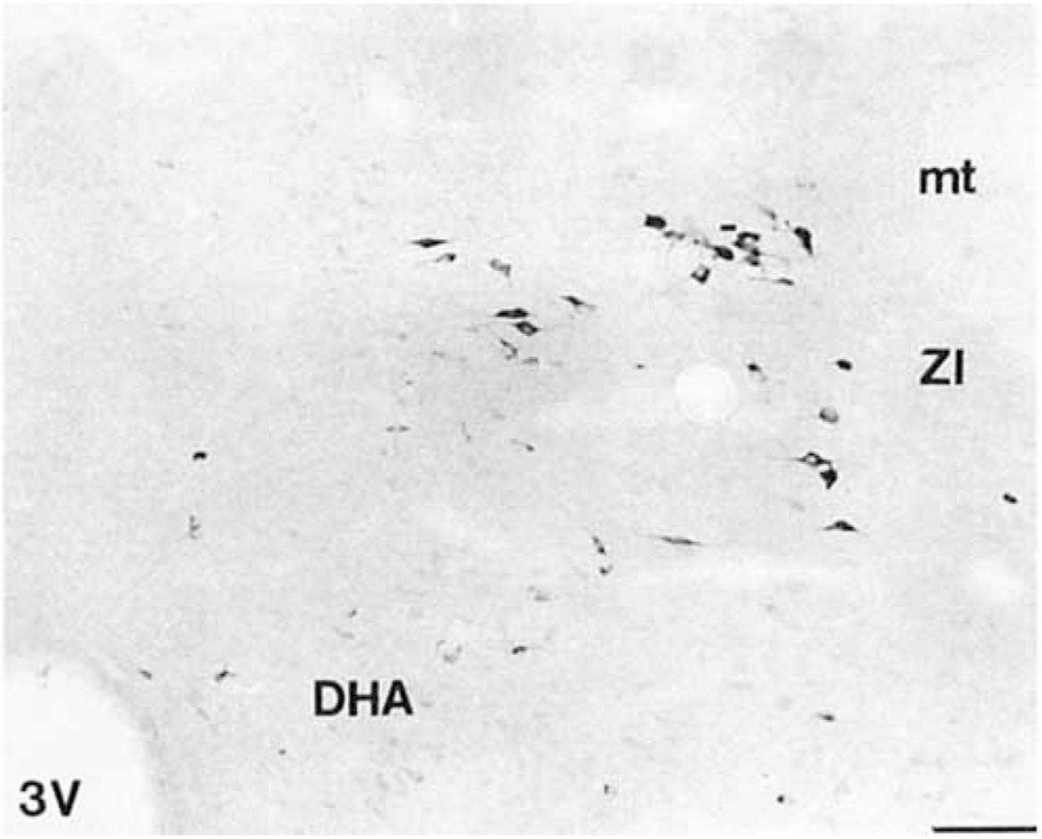

Fig. 16.
A brightfield photomicrograph shows COX 2-ir neurons ventromedial to the mammillothalamic tract in the zona incerta and dorsal hypothalamic area. Scale bar = 150 μm.

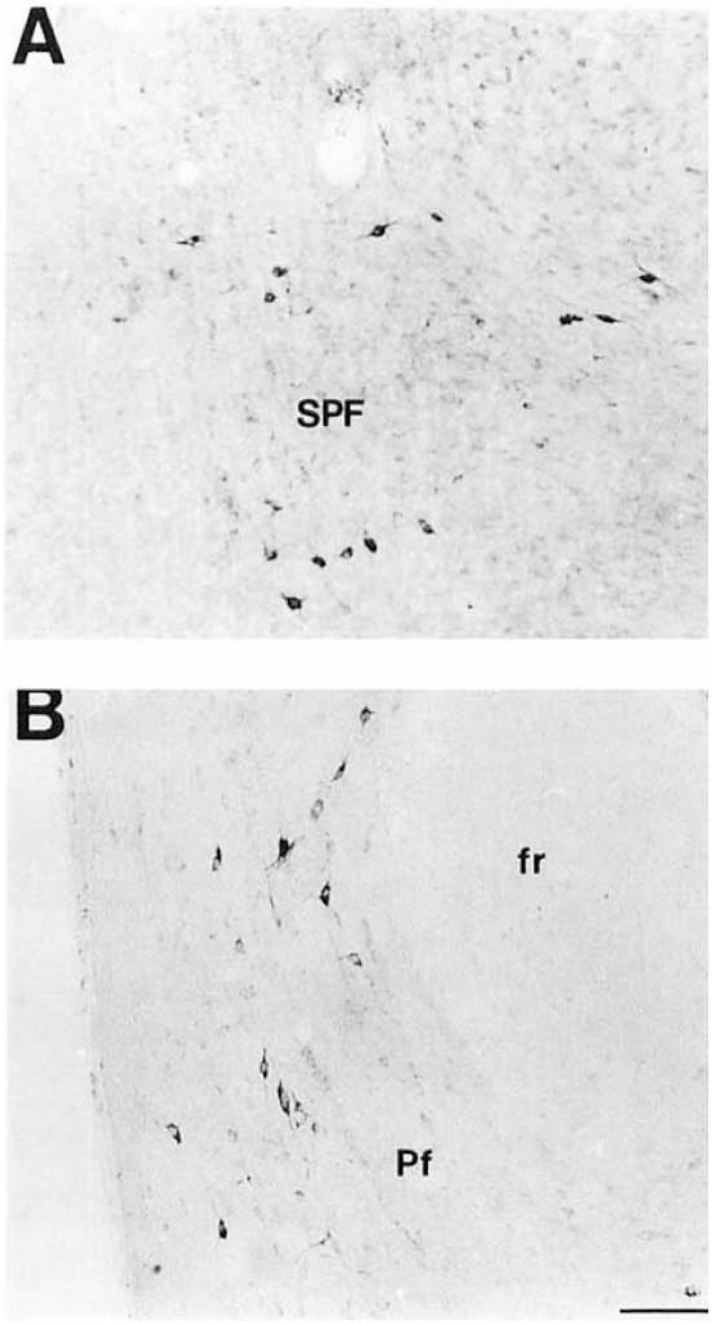

Fig. 17.

A pair of hrightfield photomicrographs depict the COX 2-ir neurons in the medial thalamus. **A:** At intermediate levels of this group, the cells outlined the magnocellular division of the subparafascicular nucleus. **B:** Caudally, this group extended dorsally through the diencephalic central gray. Scale bar = 150 μm.

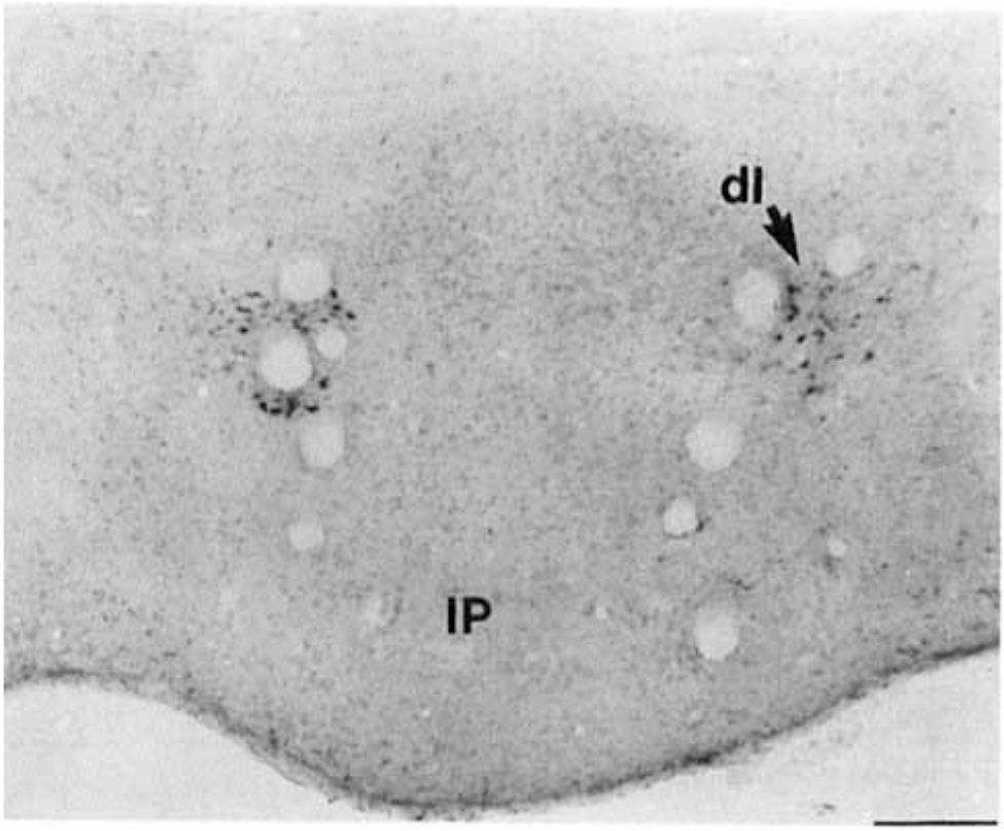

Fig. 18.

A low-power photomicrograph shows COX 2-ir neurons in the interpeduncular nucleus. Within this structure, these cells were only observed in the dorsal lateral subnucleus. Scale bar = 150 μm.

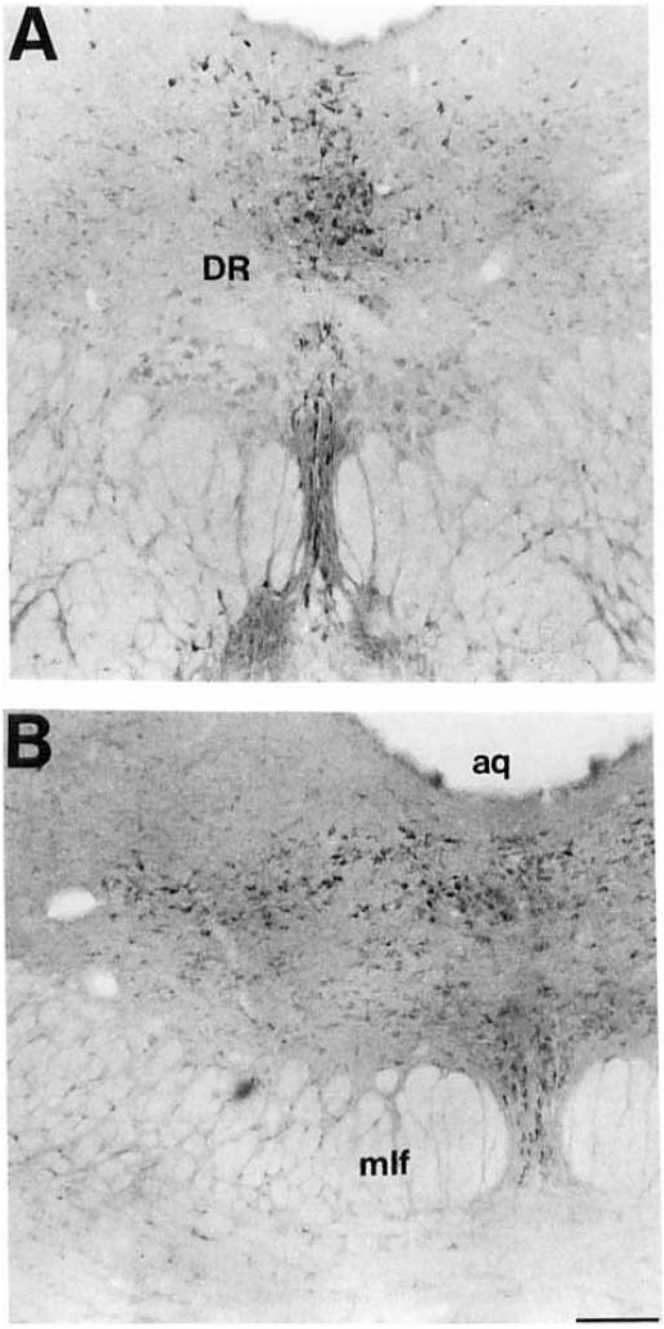

Fig. 19.

A pair of brightfield photomicrographs depict COX 2-ir neurons in the dorsal raphe nucleus. **A:** A brightfield photomicrograph depicts COX 2-ir neurons in the rostral dorsal and ventral portions of the dorsal raphe nucleus. **B:** A brightfield photomicrograph depicts COX 2-ir neurons in the caudal dorsal, ventral, and lateral portions of the dorsal raphe nucleus. Scale bar = 150 μm.

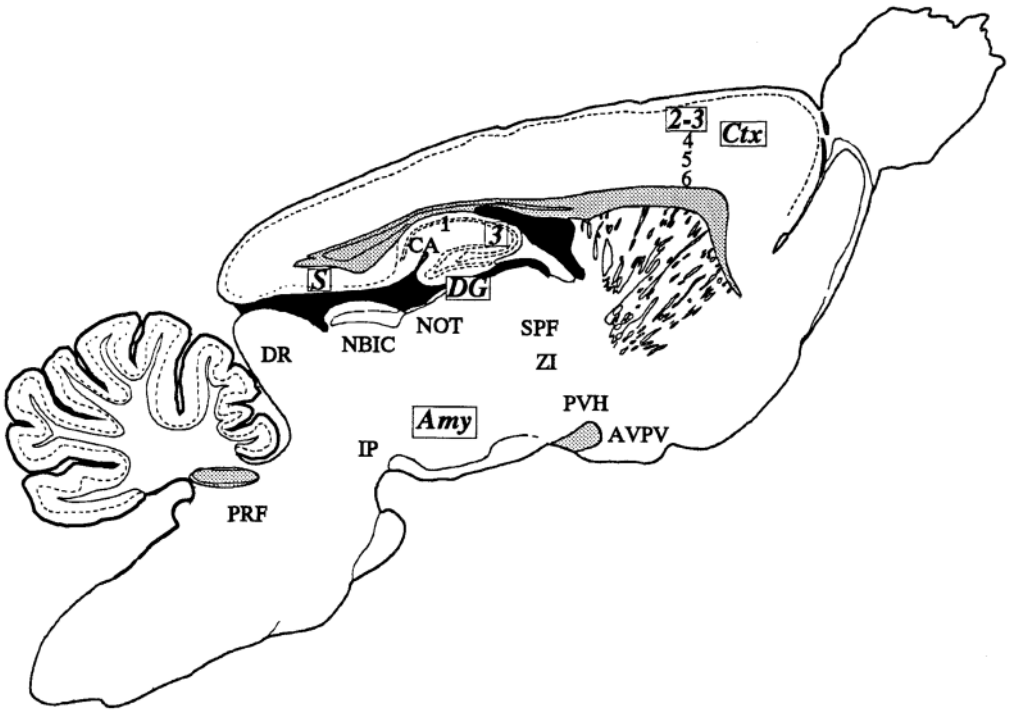

Fig. 20.

Schematic diagram shows the distribution of COX 2-ir neurons in the rat brain. Regions noted in bold and italic type with boxed abbreviations had the densest and most intensely staining COX 2-ir neurons. Other regions noted here had more modest numbers of relatively lighter stained COX 2-ir neurons. Stippled regions represent major fiber tracts in the central nervous system (CNS) and are meant to serve as anatomical landmarks.

TABLE 1

A Comparison of COX Systems in the Central Nervous System

Area	COX 1: Ovine brain[1]	COX 2: Rat brain[2]
Cortex		
Area 3B	L.4 ≫ 2/3 > 6	L.2 ≫ 4 > 5b
Area 4	L.4 and 6 > 5	L.2 ≫ 5a > 3
Area 17	L.4 > 2, 3, and 6	L.2 ≫ 4 ≫ 6
Area 18	L.4 > 2 and 3	L.2 > 3 > 4 > 5a
Insular (gran.)	L.3 and 5	L.2 ≫ 4 > 5a
Insular (dys.)	L.3 > 5	L.2 > 3/4 & 5a
Insular (agran.)	L.5	L.2/3 > 5
Infralimbic	L.2/3 > 5	L.3 ≫ 2
L. entorhinal	L.3, 5, and 6	L.2b, 3
M. entorhinal	L.5 and 6 ≫ 3	L.2
Hippocampus		
$CA_{1\text{-}4}$	s.o., CA_1 ⋙ Ca_3	s.P., CA_3 ⋙ CA_1
	s.p. *sparse* pyr. cells	s.r., $CA_{3b,c}$
Dentate gyms	g.l., ib & ob	g.l., ib & ob
	p.l., ob	p.l., ob
Subicular complex	PaS, PreS, ProS	PostS, PaS
	deep subicular pyr. cell layer	whole subicular pyr. cell layer
Amygdala	Bla ≫ Bp, BM, AAA, CoA	LA, BLp > BLa, BM
	MeA, CeA (caps.), PLCo (deep)	NLOT, PLCo (all parts), PMCo
Basal forebrain	BST, LSvl, SI, DBh, GP, CI, EN	Ø[3]
Thalamus	LGv; LGigl; SPF	SPF
Epithalamus	ZI (A13 region)	ZI (A13 region)
Hypothalamus		
Preoptic	AvPv, sparse MnPO, OVLT, LPOA, MPOA	AvPv, *dense* MnPo, OVLT
Anterior	AHA, mPVH, few dPVH	mPVH
Tuberal	DMH, DHA, VHM, ARH, PFA, LHA	Ø
Posterior	TMN, VPM, PvP	Ø
Pretectum	mPTA	NOT
Midbrain	CG, IPr, VTA, SNpr, AM, EW, CTF, Dk, SOM, PAGdl, LDT, MEA, SC. Cf. ICex	CG, IPdl
Pons	PBI, Sag, Sc, PRF	Sc
Medulla	NTS, RM, SN5sg, Cu, Gr, MRF	Ø

[1] Breder et al., 1992.

[2] Present study.

[3] Ø = no immunoreactive neurons.